Modeling Sea Ice in a Changing Climate

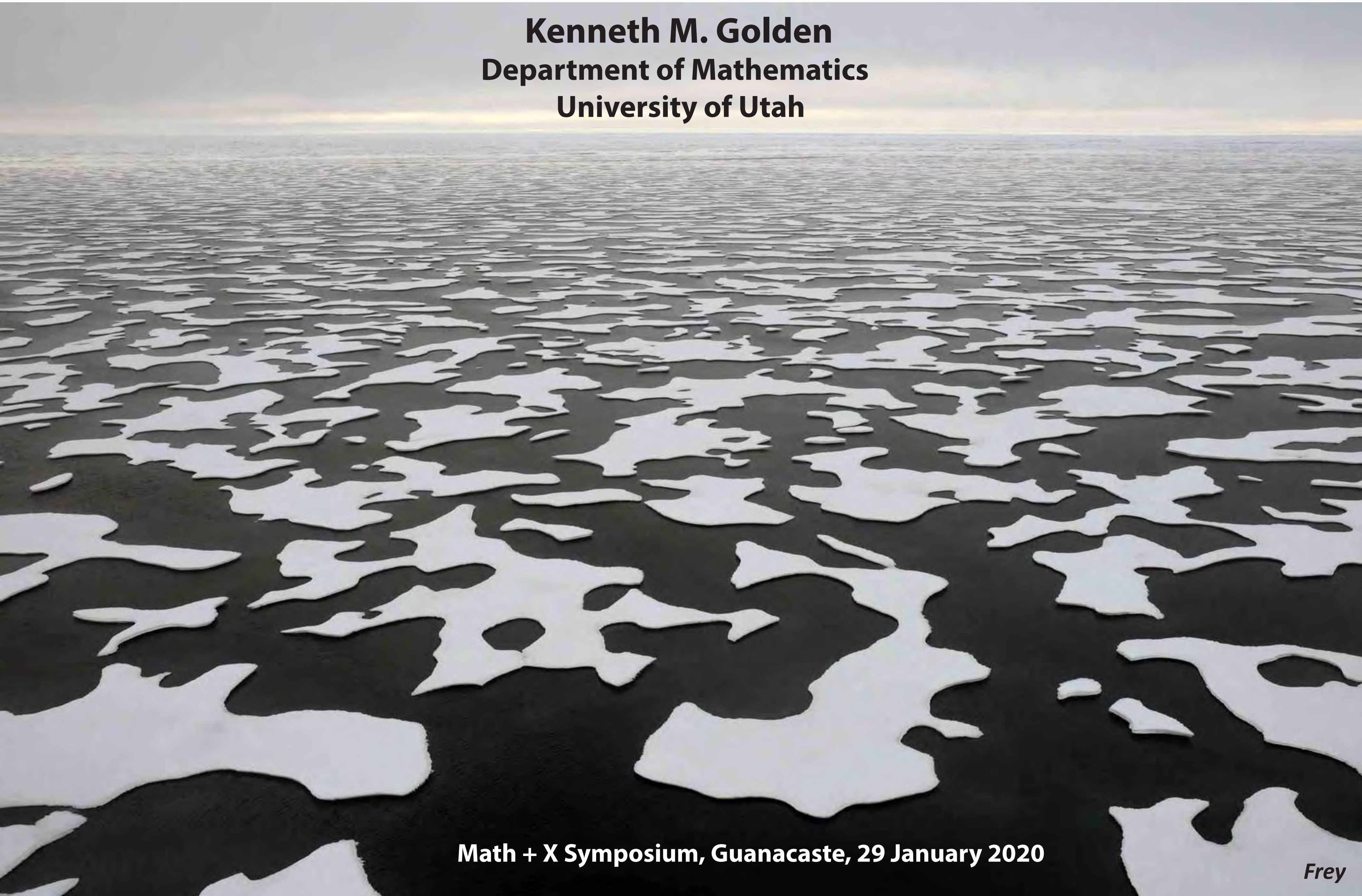

Kenneth M. Golden

Department of Mathematics

University of Utah

Math + X Symposium, Guanacaste, 29 January 2020

Frey

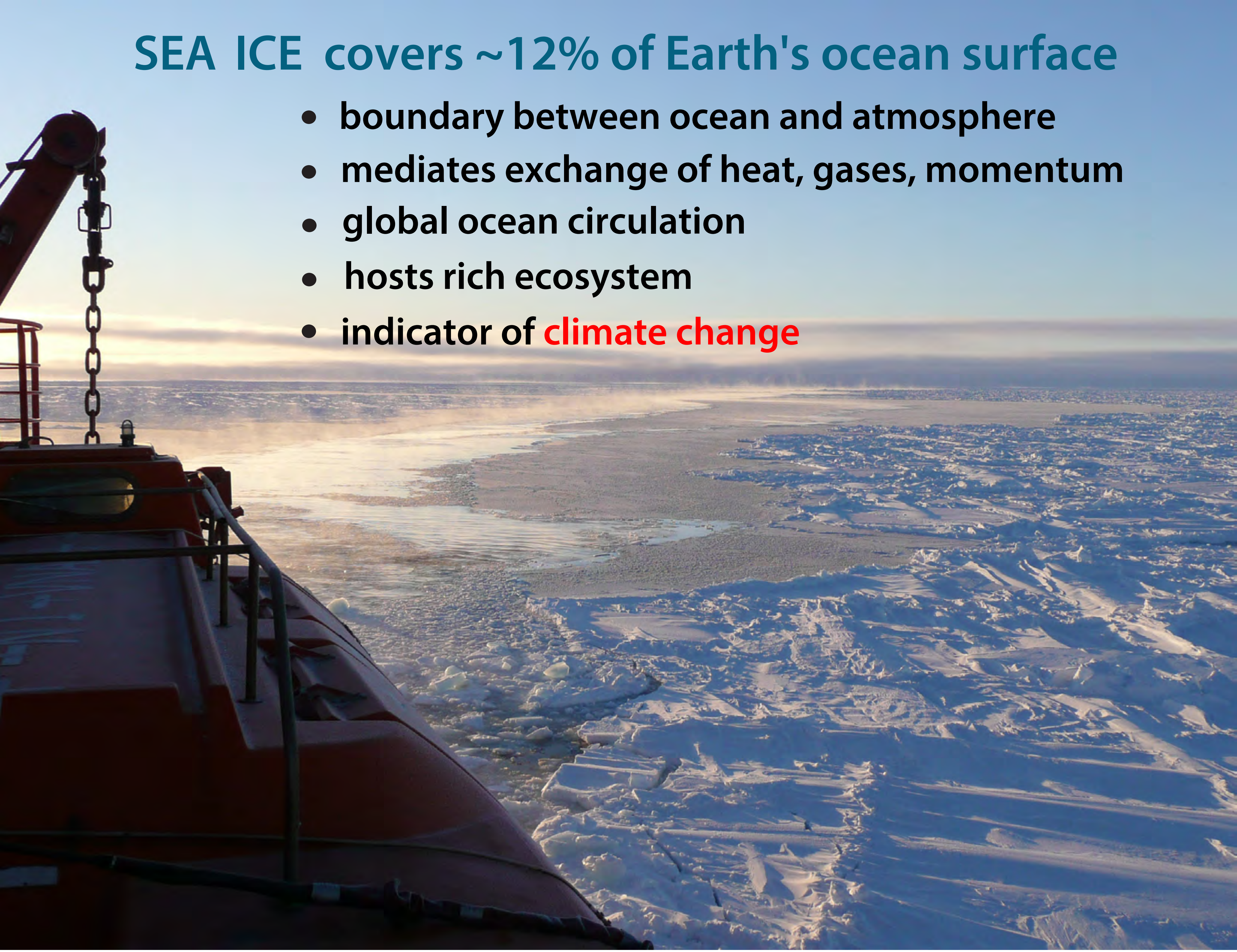

SEA ICE covers ~12% of Earth's ocean surface

- boundary between ocean and atmosphere
- mediates exchange of heat, gases, momentum
- global ocean circulation
- hosts rich ecosystem
- indicator of climate change

polar ice caps critical to global climate in reflecting incoming solar radiation

white snow and ice
reflect

Earth's refrigerator

NASA

NASA

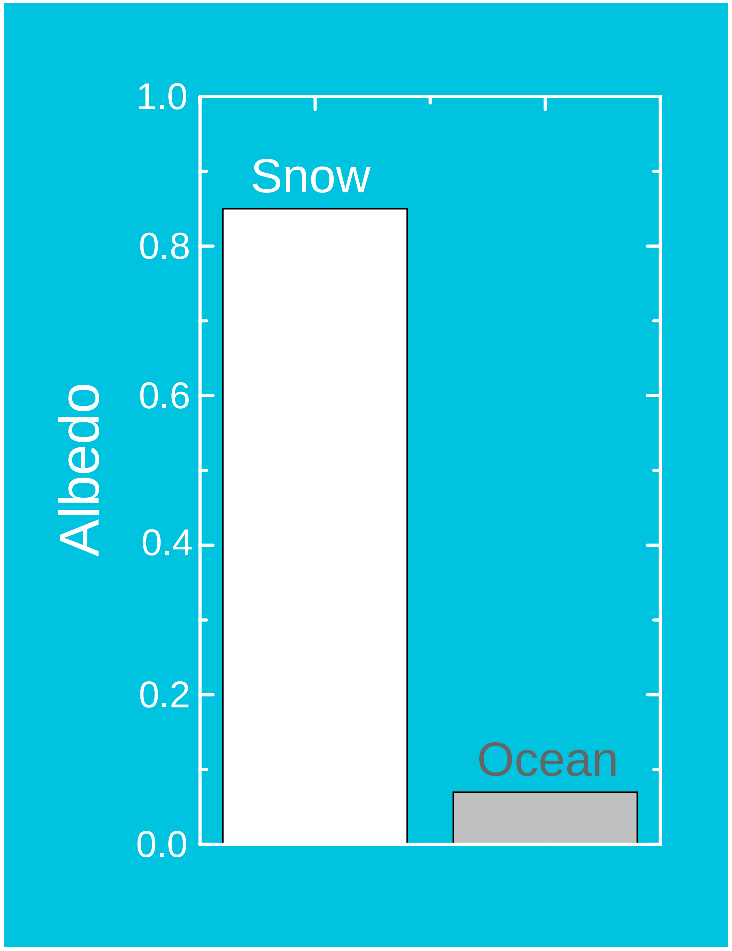

dark water and land
absorb

$$\textbf{\textit{albedo}}\ \ \alpha = \frac{\text{reflected sunlight}}{\text{incident sunlight}}$$

the summer Arctic sea ice pack is melting

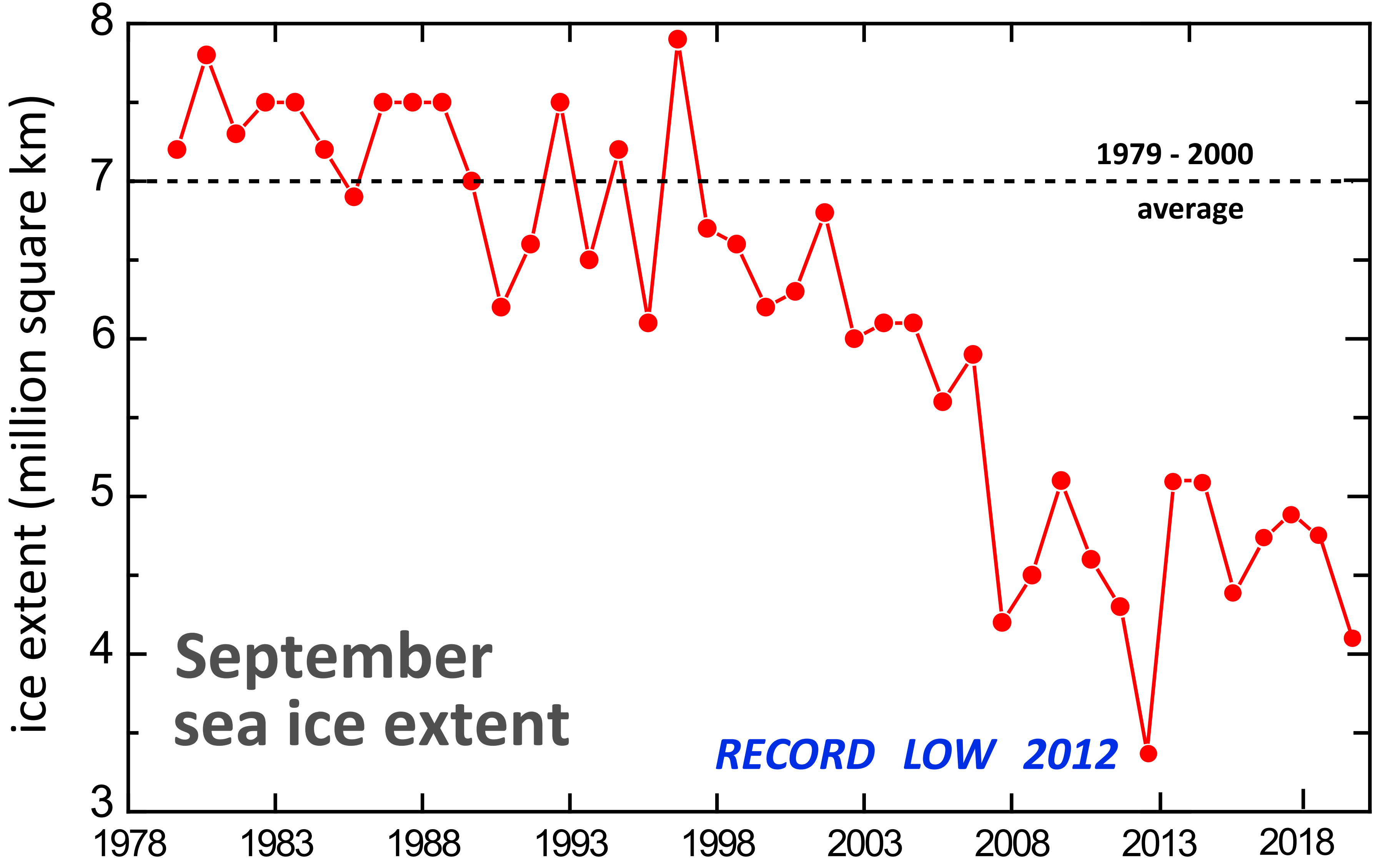

National Snow and Ice Data Center

Change in Arctic Sea Ice Extent

September 1980 -- 7.8 million km^2

September 2012 -- 3.4 million km^2

recent losses in comparison to the United States

Perovich

Arctic sea ice decline:
faster than predicted by climate models

Stroeve et al., GRL, 2007

Stroeve et al., GRL, 2012

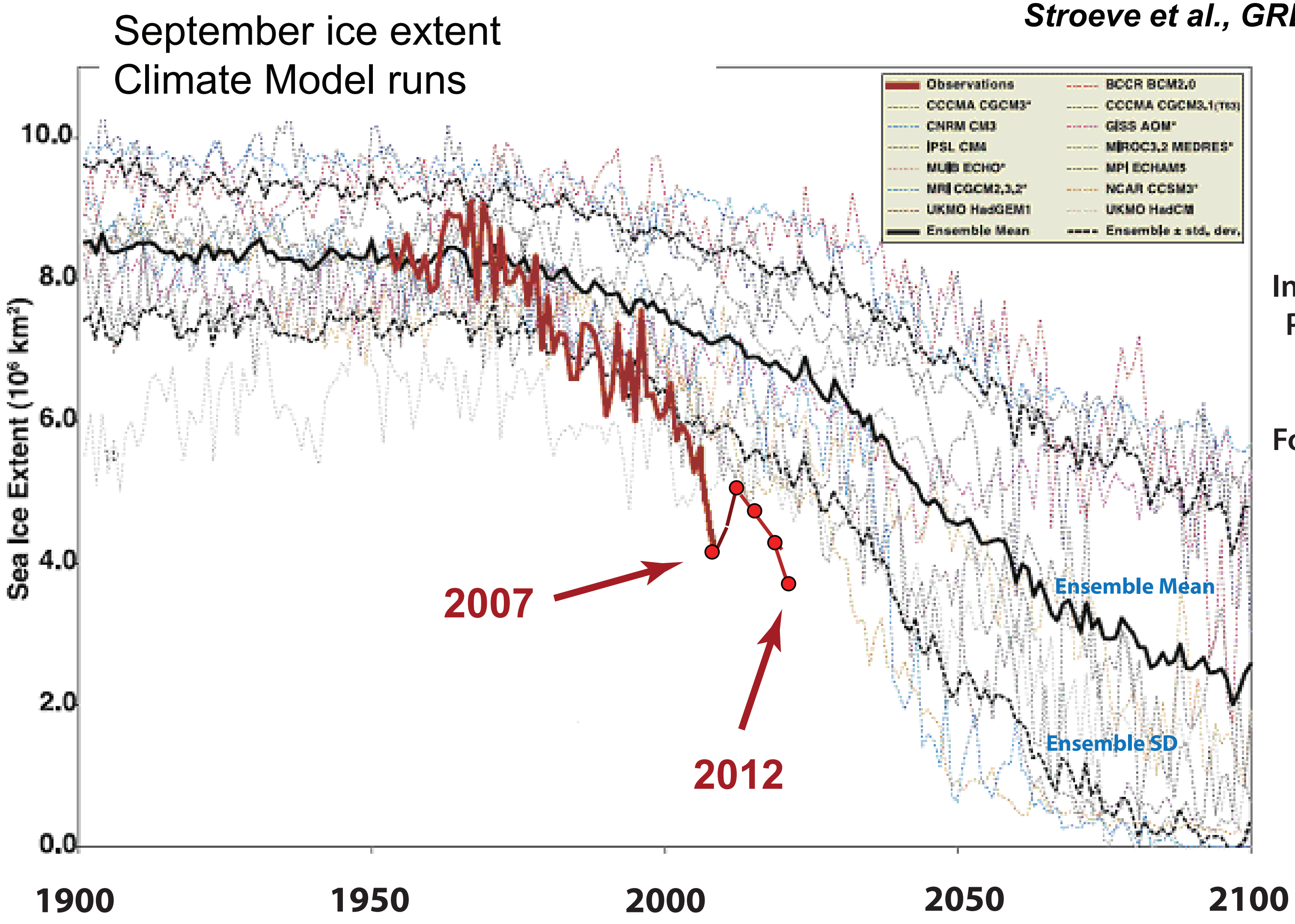
September ice extent
Climate Model runs

IPCC AR4 Models

Intergovernmental
Panel on Climate
Change (IPCC)

Fourth Assessment
AR4, 2007

challenge

represent sea ice more realistically in climate models

account for key processes

such as melt pond evolution

How do patterns of dark and light evolve?

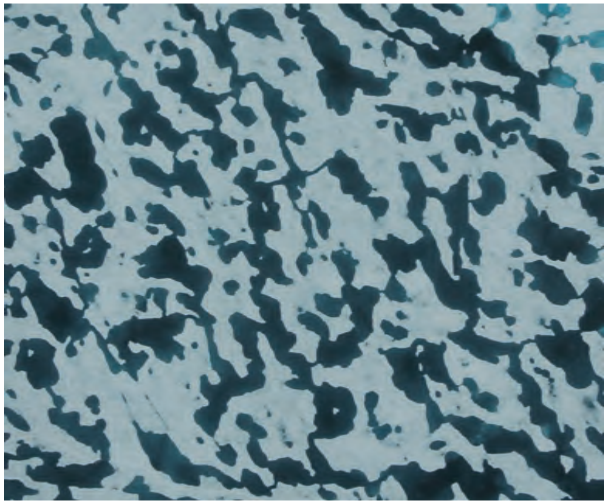

Impact of melt ponds on Arctic sea ice simulations from 1990 to 2007

Flocco, Schroeder, Feltham, Hunke, JGR Oceans 2012

For simulations with ponds September ice volume is nearly 40% lower.

... and other sub-grid scale structures and processes

linkage of scales

Sea Ice is a Multiscale Composite Material

sea ice microstructure

brine inclusions

Weeks & Assur 1969

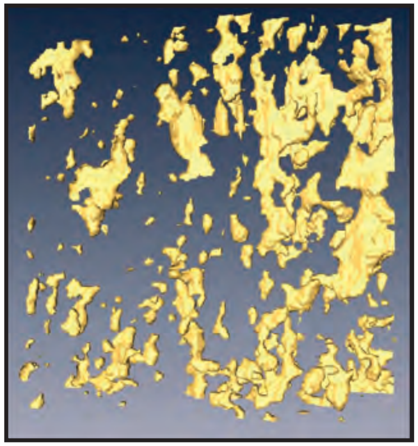

H. Eicken

Golden *et al. GRL* 2007

polycrystals

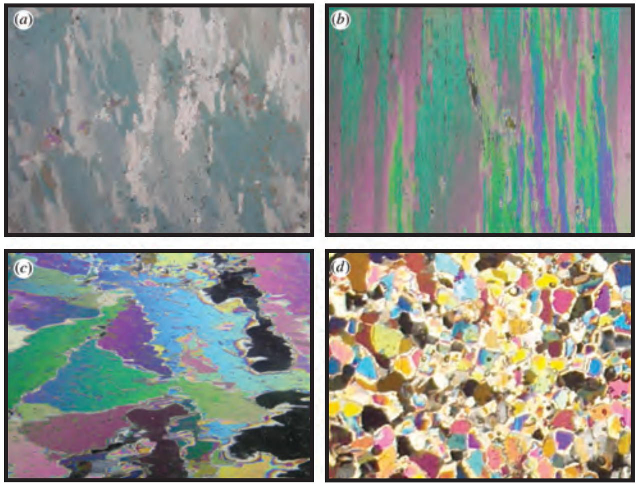

Gully *et al. Proc. Roy. Soc. A* 2015

brine channels

D. Cole

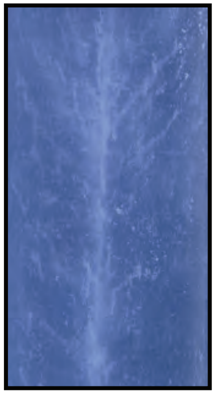

K. Golden

millimeters

centimeters

---

sea ice mesostructure

sea ice macrostructure

Arctic melt ponds

K. Frey

Antarctic pressure ridges

K. Golden

sea ice floes

J. Weller

sea ice pack

NASA

meters

kilometers

What is this talk about?

the role of microstructure in determining effective properties

Use **statistical physics and homogenization for composites** to LINK SCALES in the sea ice system ... compute effective behavior on scales relevant to coarse-grained climate models, remote sensing, process studies, ...

A tour of Herglotz functions in the study of sea ice and its role in climate.

1. ***Sea ice microphysics and fluid transport***
2. ***Analytic Continuation Method, integral representations***
3. ***Extension to polycrystals, advection diffusion, waves in sea ice***
4. ***Fractal geometry of melt pond evolution***

Solving problems in physics of sea ice drives advances in theory of composite materials.

cross - pollination

Forward and Inverse HOMOGENIZATION for Composites

LINKING SCALES

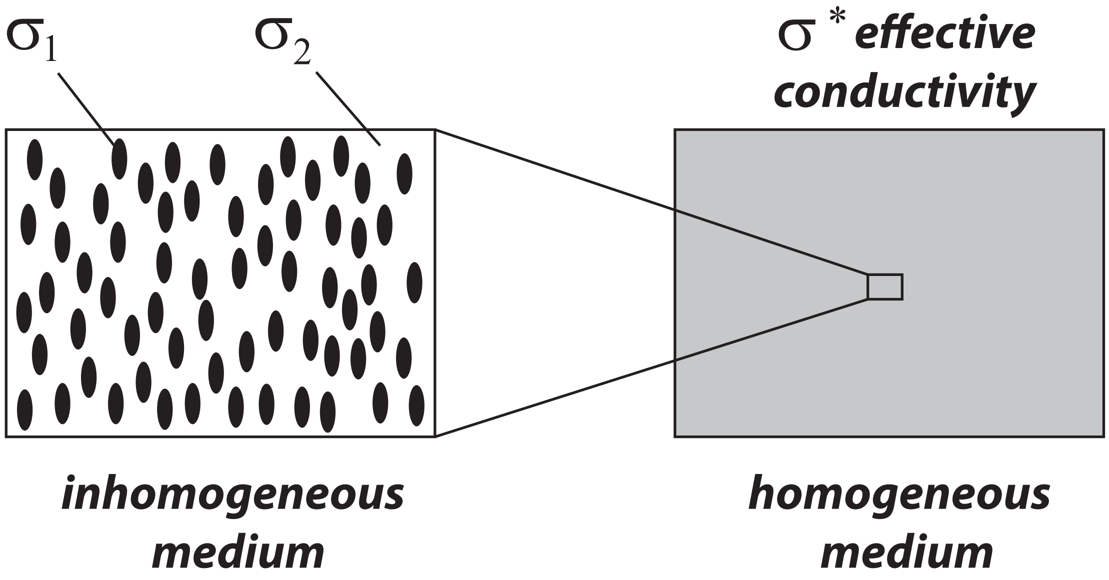

FORWARD

INVERSE

find the homogeneous medium which behaves macroscopically the same as the inhomogeneous medium

find the microstructure which gives rise to observed or desired effective behavior

Maxwell 1873 : effective conductivity of a dilute suspension of spheres
Einstein 1906 : effective viscosity of a dilute suspension of rigid spheres in a fluid

Wiener 1912 : arithmetic and harmonic mean bounds on effective conductivity
Hashin and Shtrikman 1962 : variational bounds on effective conductivity

widespread use of composites in late 20th century due in large part to advances in mathematically predicting their effective properties

How do scales interact in the sea ice system?

NASA

basin scale -
grid scale
albedo

Linking Scales

km
scale
melt
ponds

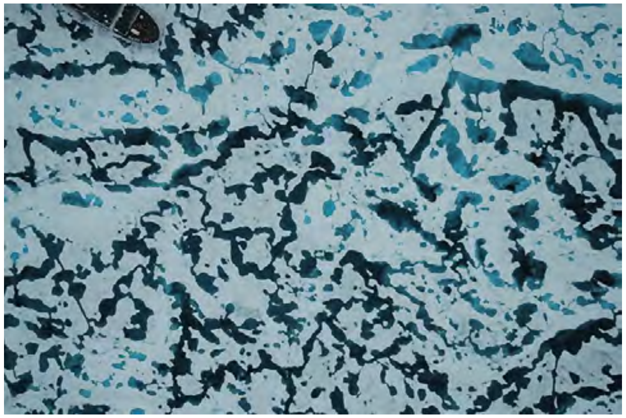

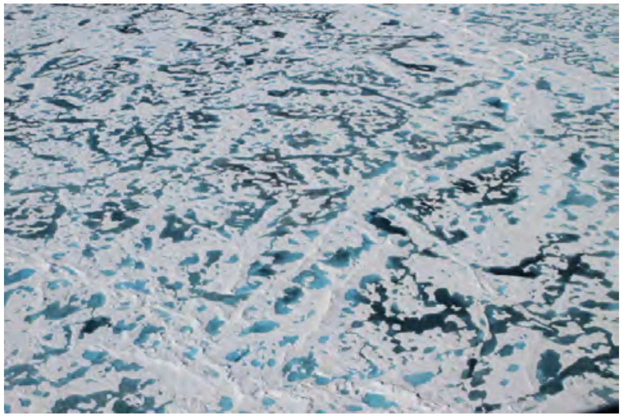

Perovich

km
scale
melt
ponds

Linking Scales

mm
scale
brine
inclusions

meter
scale
snow
topography

sea ice microphysics

fluid transport

fluid flow through the porous microstructure of sea ice governs key processes in polar climate and ecosystems

evolution of Arctic melt ponds and sea ice albedo

K. Golden

nutrient flux for algal communities

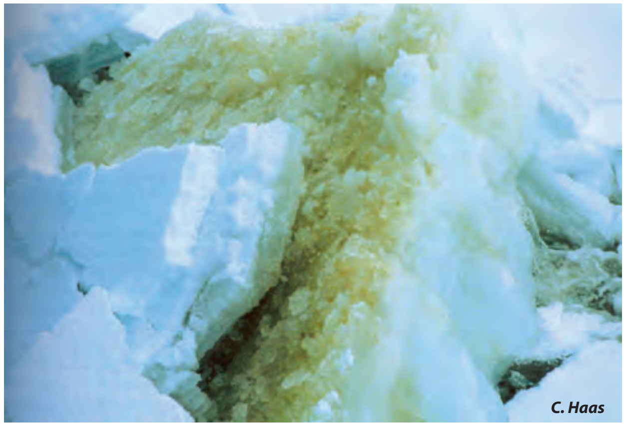

C. Haas

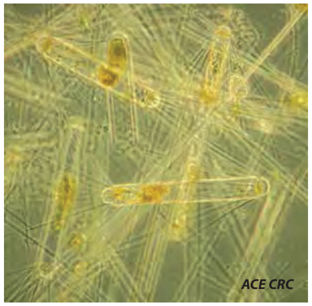

ACE CRC

C. Krembs

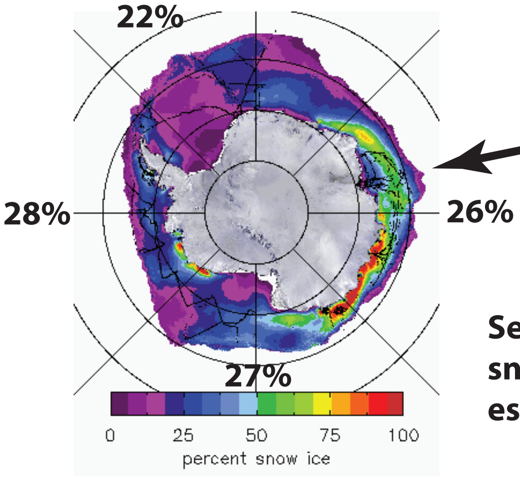

T. Maksym and T. Markus, 2008

September snow-ice estimates

Antarctic surface flooding and snow-ice formation

- *evolution of salinity profiles*
- *ocean-ice-air exchanges of heat, CO_2*

fluid permeability of a porous medium

how much water gets
through the sample
per unit time?

Darcy's Law

for slow viscous flow in a porous medium

averaged
fluid velocity

pressure
gradient

$$\mathrm{v} = -\frac{\mathbf{k}}{\eta}\nabla p$$

viscosity

$\mathbf{k}$ = fluid permeability tensor

HOMOGENIZATION

mathematics for analyzing effective behavior of heterogeneous systems

Critical behavior of fluid transport in sea ice

Arctic field data

vertical fluid permeability k (m^2)

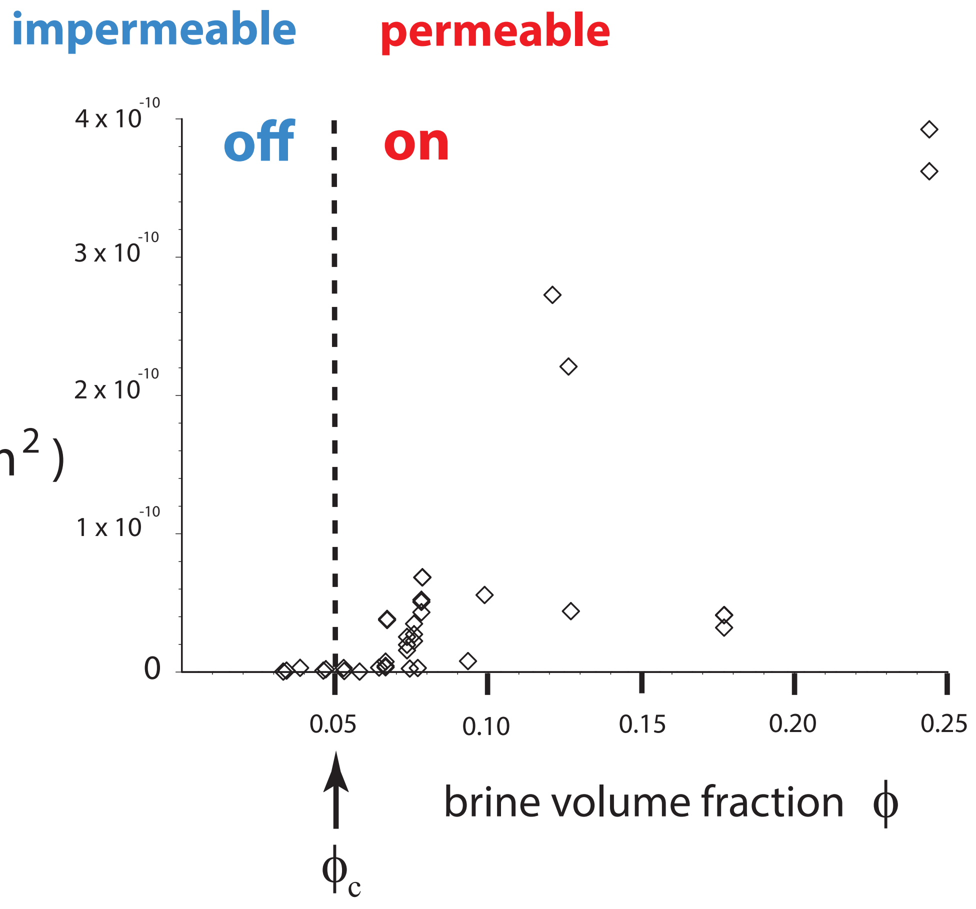

"on - off" switch for fluid flow

critical brine volume fraction $\phi_c \approx 5\%$ ⟷ $T_c \approx -5^\circ\text{C}, \; S \approx 5$ ppt

RULE OF FIVES

Golden, Ackley, Lytle Science 1998
Golden, Eicken, Heaton, Miner, Pringle, Zhu GRL 2007
Pringle, Miner, Eicken, Golden J. Geophys. Res. 2009

percolation theory

probabilistic theory of connectedness

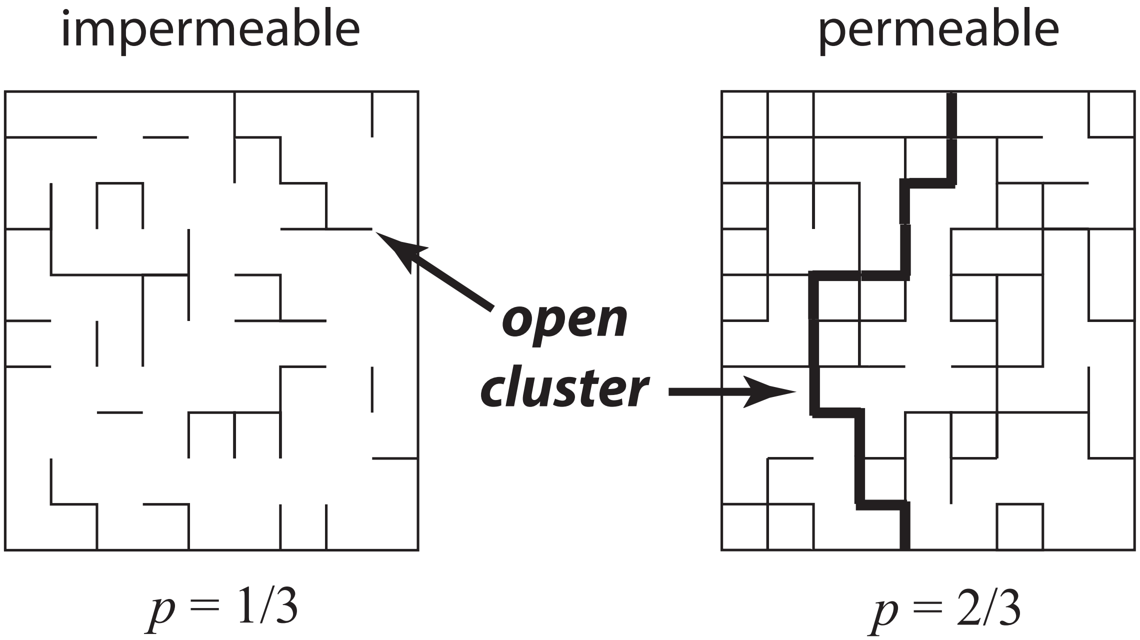

bond → ***open*** *with probability* p
closed *with probability* $1-p$

percolation threshold

$$p_c = 1/2 \quad \text{for} \quad d = 2$$

smallest *p* for which there is an infinite open cluster

Continuum percolation model for ***stealthy*** materials applied to sea ice microstructure explains **Rule of Fives** and Antarctic data on ice production and algal growth

$\phi_c \approx 5\ \%$ Golden, Ackley, Lytle, *Science*, 1998

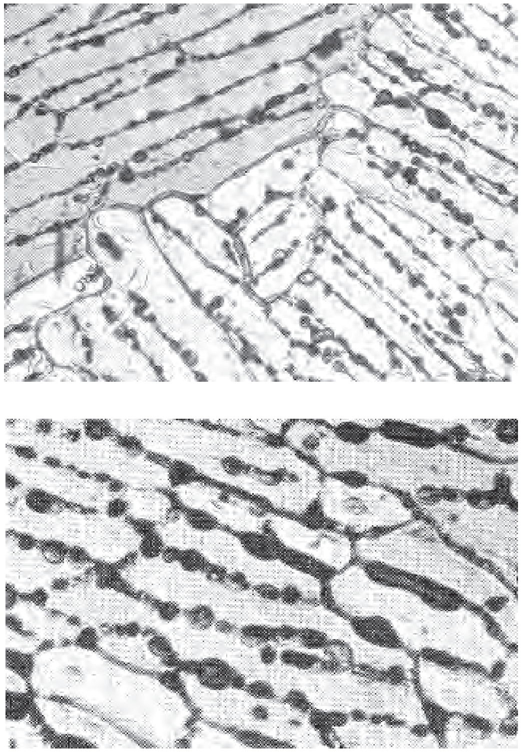

sea ice

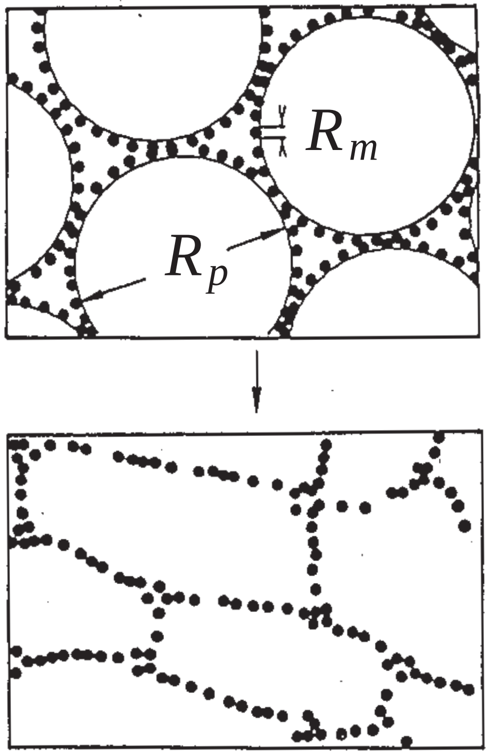

compressed powder

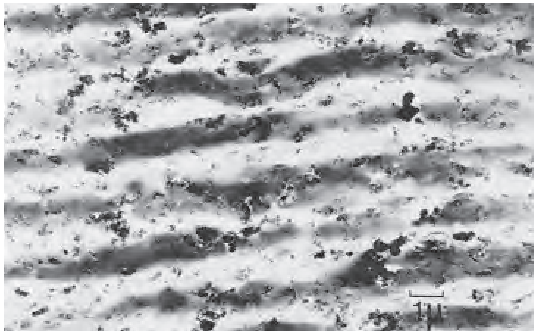

radar absorbing composite

sea ice is radar absorbing

Thermal evolution of permeability and microstructure in sea ice

Golden, Eicken, Heaton, Miner, Pringle, Zhu, Geophysical Research Letters 2007

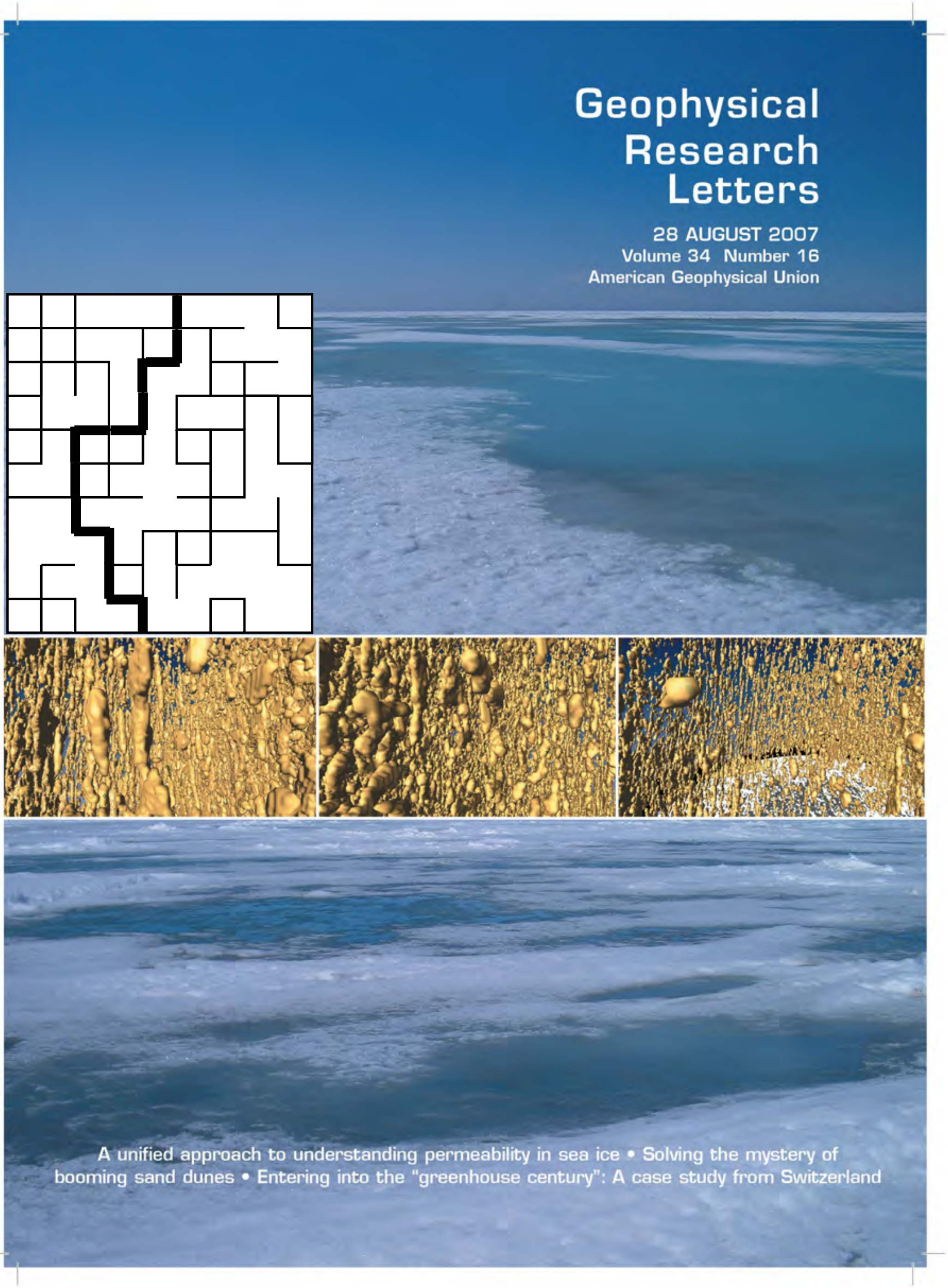

Geophysical Research Letters

28 AUGUST 2007
Volume 34 Number 16
American Geophysical Union

A unified approach to understanding permeability in sea ice • Solving the mystery of booming sand dunes • Entering into the "greenhouse century": A case study from Switzerland

micro-scale

controls

macro-scale

processes

percolation theory

$$k(\phi) = k_0(\phi - 0.05)^2 \longleftarrow$$

critical exponent

t

$$k_0 = 3 \text{ x } 10^{-8} \text{ m}^2$$

hierarchical model

network model

rigorous bounds

agree closely with
field data

X-ray tomography for brine inclusions

unprecedented look at thermal evolution of brine phase and its connectivity

confirms rule of fives

Pringle, Miner, Eicken, Golden
J. Geophys. Res. 2009

brine volume fraction and ***connectivity*** increase with temperature

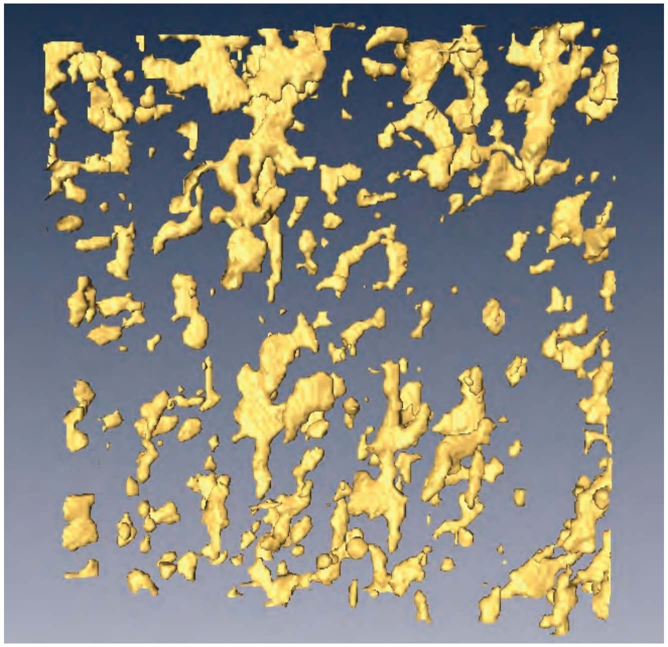

$T = -15\,^\circ\mathrm{C}, \ \phi = 0.033$

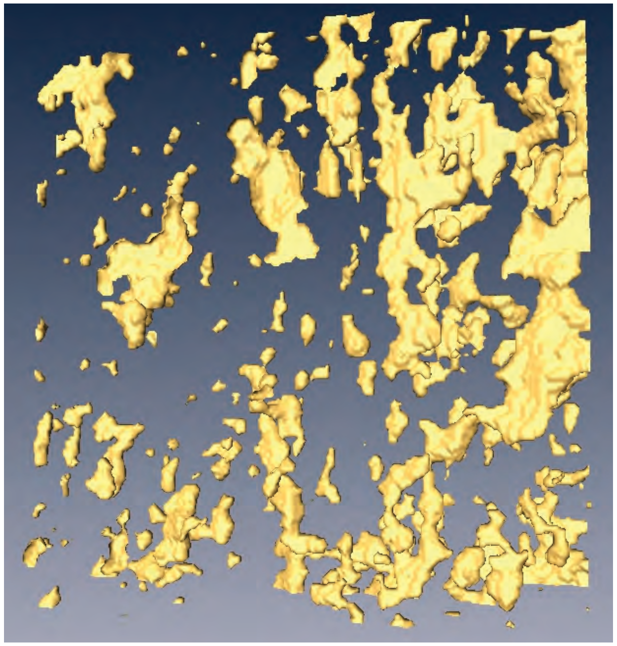

$T = -6\,^\circ\mathrm{C}, \ \phi = 0.075$

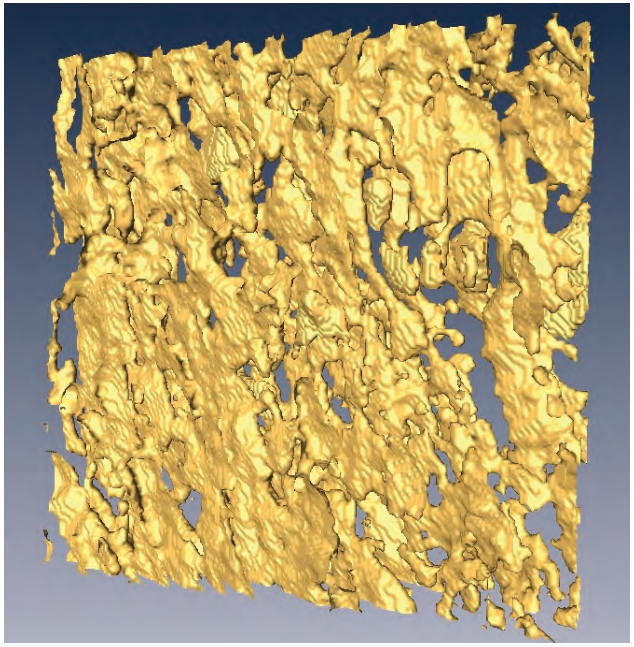

$T = -3\,^\circ\mathrm{C}, \ \phi = 0.143$

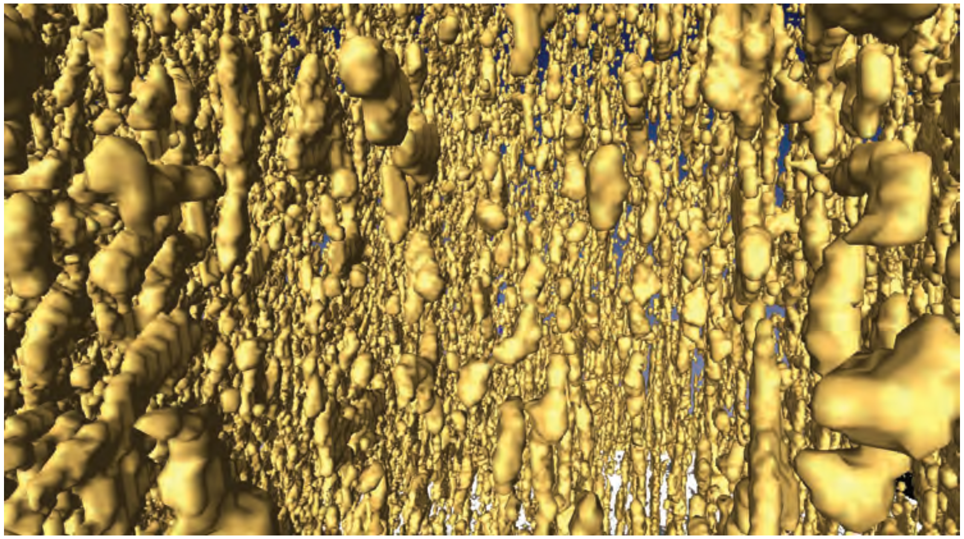

$T = -8\,^\circ\mathrm{C}, \ \phi = 0.057$

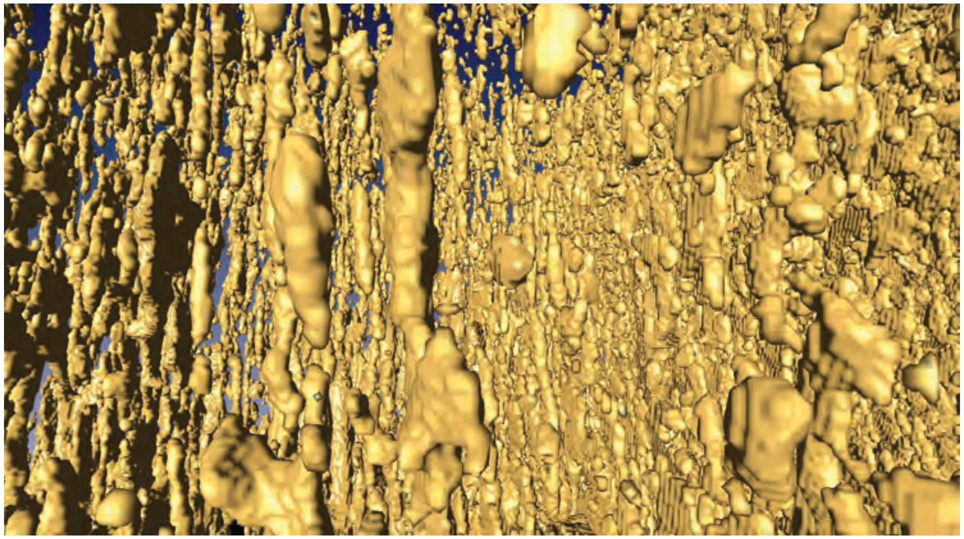

$T = -4\,^\circ\mathrm{C}, \ \phi = 0.113$

X-ray tomography for brine in sea ice

Golden *et al.*, *Geophysical Research Letters*, 2007

Sea ice algae secrete extracellular polymeric substances (EPS) affecting evolution of brine microstructure.

How does EPS affect fluid transport?

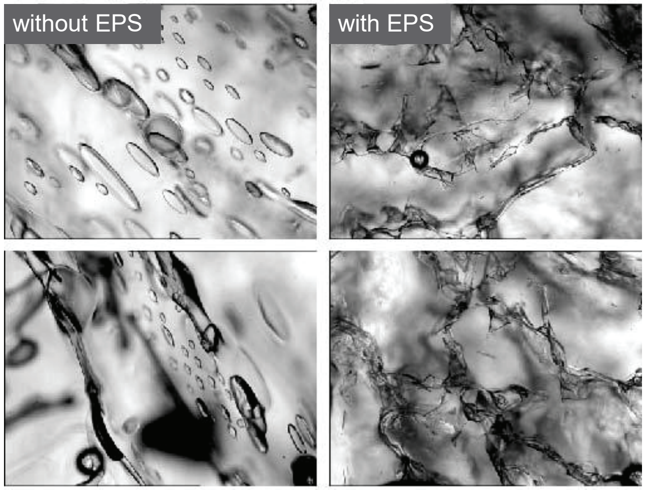

Krembs, Eicken, Deming, PNAS 2011

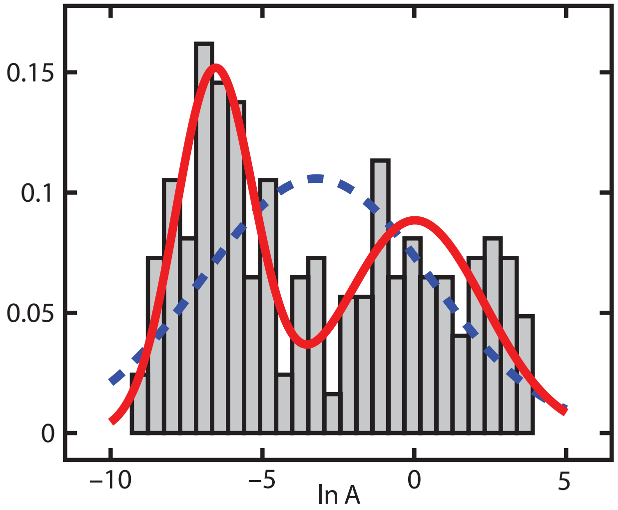

RANDOM PIPE MODEL

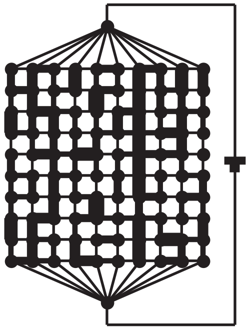

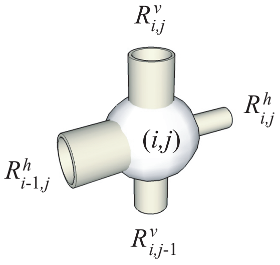

Zhu, Jabini, Golden,
Eicken, Morris
Ann. Glac. 2006

- **Bimodal** lognormal distribution for brine inclusions
- Develop random pipe network model with bimodal distribution;
  Use numerical methods that can handle larger variances in sizes.
- Results predict observed drop in fluid permeability *k*.
- **Rigorous bound on *k* for bimodal distribution of pore sizes**

Steffen, Epshteyn, Zhu, Bowler, Deming, Golden
Multiscale Modeling and Simulation, 2018

How does the biology affect the physics?

ISSN 0002-9920

Notices

of the American Mathematical Society

May 2009

Volume 56, Number 5

Climate Change and the Mathematics of Transport in Sea Ice

page 562

Mathematics and the Internet: A Source of Enormous Confusion and Great Potential

page 586

Real analysis in polar coordinates (see page 613)

photo by Jan Lieser

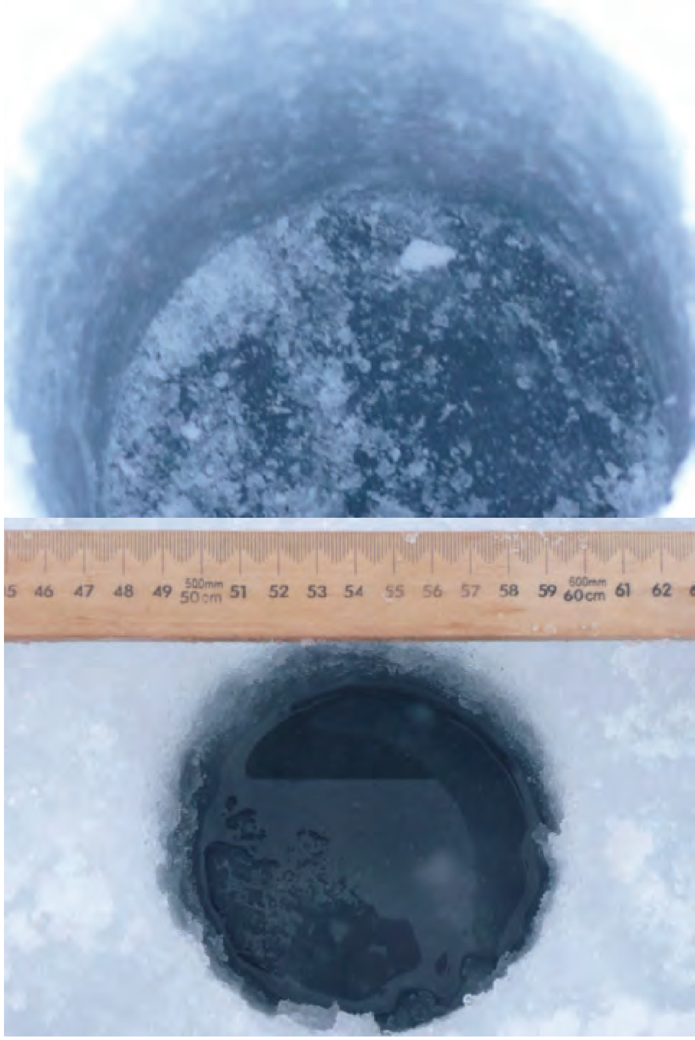

measuring
fluid permeability
of Antarctic sea ice

SIPEX 2007

Remote sensing of sea ice

sea ice thickness
ice concentration

INVERSE PROBLEM

Recover sea ice properties from electromagnetic (EM) data

ε^*

effective complex permittivity
(dielectric constant, conductivity)

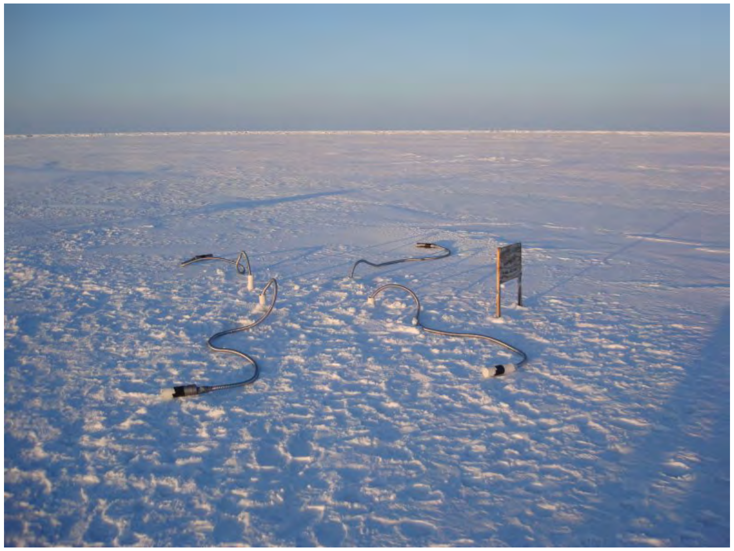

brine volume fraction
brine inclusion connectivity

Effective complex permittivity of a two phase composite in the quasistatic (long wavelength) limit

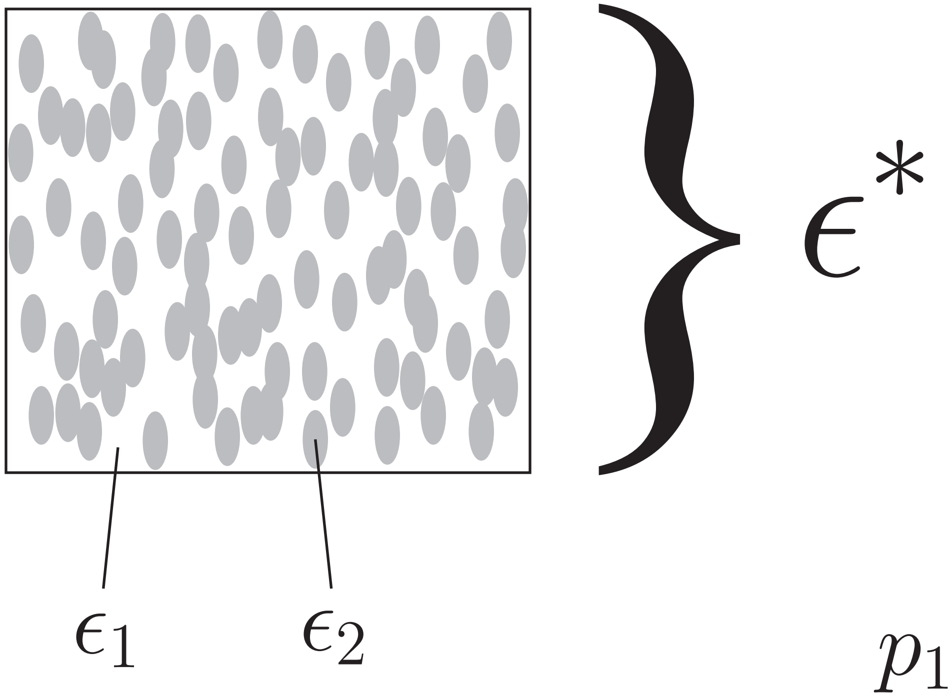

$$D = \epsilon E$$

$$\nabla \cdot D = 0$$

$$\nabla \times E = 0$$

$$\langle D \rangle = \epsilon^* \langle E \rangle$$

p_1 , p_2 = volume fractions of the components

$$\epsilon^* = \epsilon^* \left(\frac{\epsilon_1}{\epsilon_2} \; , \text{ composite geometry } \right)$$

What are the effective propagation characteristics of an EM wave (radar, microwaves) in the medium?

Analytic Continuation Method for Homogenization

Bergman (1978), Milton (1979), Golden and Papanicolaou (1983), Theory of Composites, Milton (2002)

Stieltjes integral representation for homogenized parameter

separates geometry from parameters

geometry

$$F(s) = 1 - \frac{\epsilon^*}{\epsilon_2} = \int_0^1 \frac{d\mu(z)}{s-z}$$

material parameters

$$s = \frac{1}{1 - \epsilon_1 / \epsilon_2}$$

μ

- spectral measure of self adjoint operator $\Gamma\chi$
- mass = p_1
- higher moments depend on n-point correlations

$$\Gamma = \nabla(-\Delta)^{-1}\nabla\cdot$$

$\chi =$ characteristic function of the brine phase

$$E = s\,(s + \Gamma\chi)^{-1} e_k$$

$\Gamma\chi$: microscale $\longrightarrow$ macroscale

$\Gamma\chi$ *links scales*

Golden and Papanicolaou, Comm. Math. Phys. 1983

forward and inverse bounds on the complex permittivity of sea ice

forward bounds

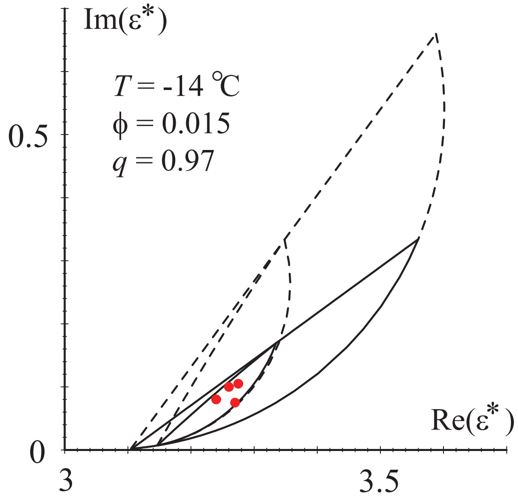

4.75 GHz data

matrix particle

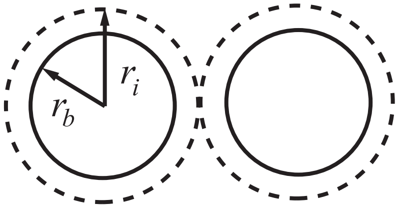

$$q = r_b / r_i$$

$$0 < q < 1$$

Golden 1995, 1997

inverse bounds

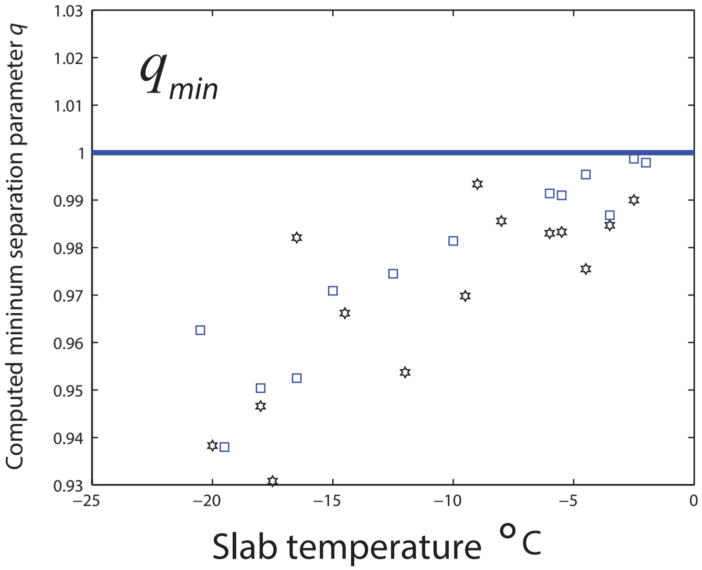

Inverse Homogenization

Cherkaev and Golden (1998), Day and Thorpe (1999), Cherkaev (2001), McPhedran, McKenzie, Milton (1982), *Theory of Composites*, Milton (2002)

$\varepsilon^* \longrightarrow$ ***composite geometry***
(spectral measure μ)

inverse bounds and recovery of brine porosity

Gully, Backstrom, Eicken, Golden
Physica B, 2007

inversion for brine inclusion separations in sea ice from measurements of effective complex permittivity ε^*

rigorous inverse bound
on spectral gap

construct algebraic curves which bound admissible region in (p,q)-space

Orum, Cherkaev, Golden
Proc. Roy. Soc. A, 2012

SEA ICE

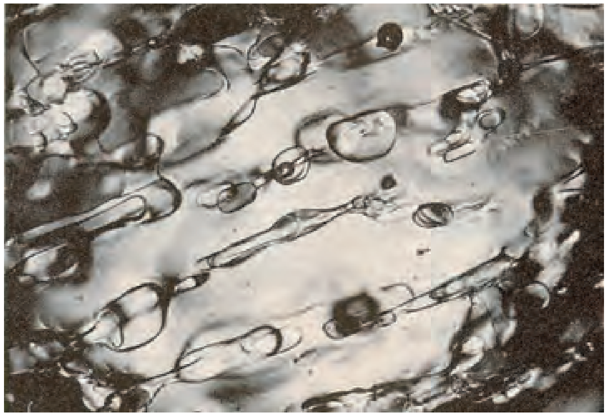

HUMAN BONE

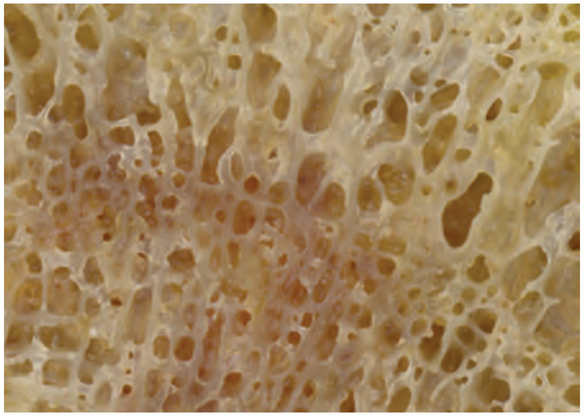

spectral characterization of porous microstructures in human bone

young healthy trabecular bone

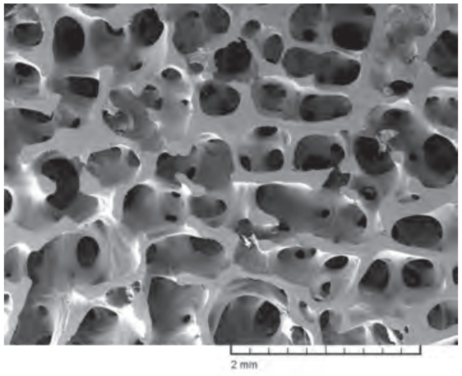

old osteoporotic trabecular bone

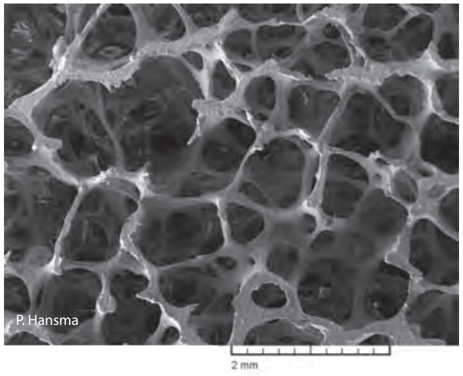

reconstruct spectral measures from complex permittivity data

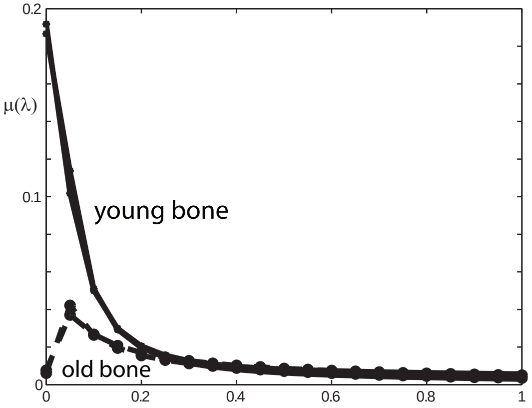

use regularized inversion scheme

apply spectral measure analysis of brine connectivity and spectral inversion to electromagnetic monitoring of osteoporosis

Golden, Murphy, Cherkaev, J. Biomechanics 2011

the math doesn't care if it's sea ice or bone!

direct calculation of spectral measures

Murphy, Hohenegger, Cherkaev, Golden, *Comm. Math. Sci.* 2015

- depends only on the composite geometry
- discretization of microstructural image gives binary network
- fundamental operator becomes a random matrix
- spectral measure computed from eigenvalues and eigenvectors

once we have the spectral measure μ it can be used in Stieltjes integrals for other transport coefficients:

electrical and thermal conductivity, complex permittivity, magnetic permeability, diffusion, fluid flow properties

earlier studies of spectral measures

Day and Thorpe 1996
Helsing, McPhedran, Milton 2011

Spectral statistics for 2D random resistor network

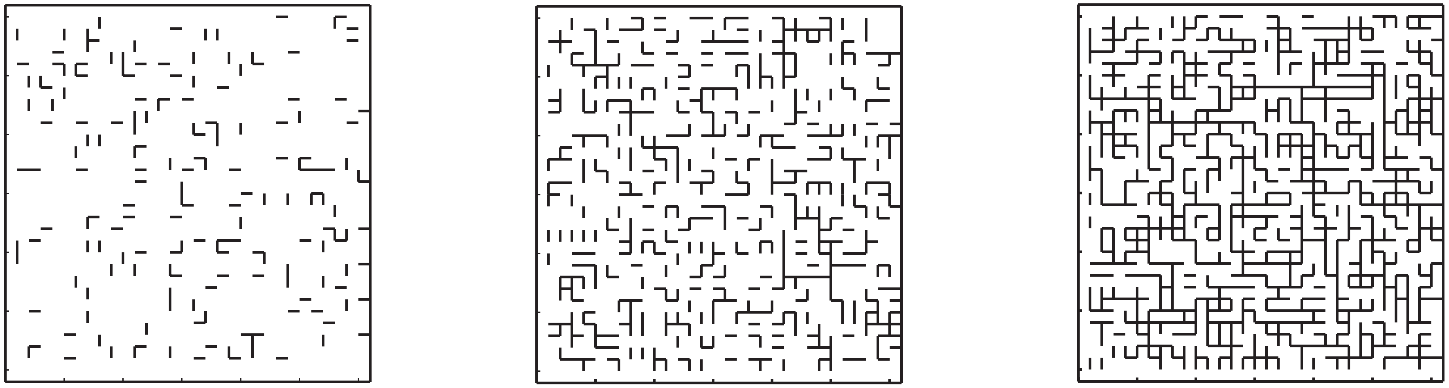

Spectral Measures

Murphy and Golden, *J. Math. Phys.*, 2012
Murphy et al. *Comm. Math. Sci.*, 2015

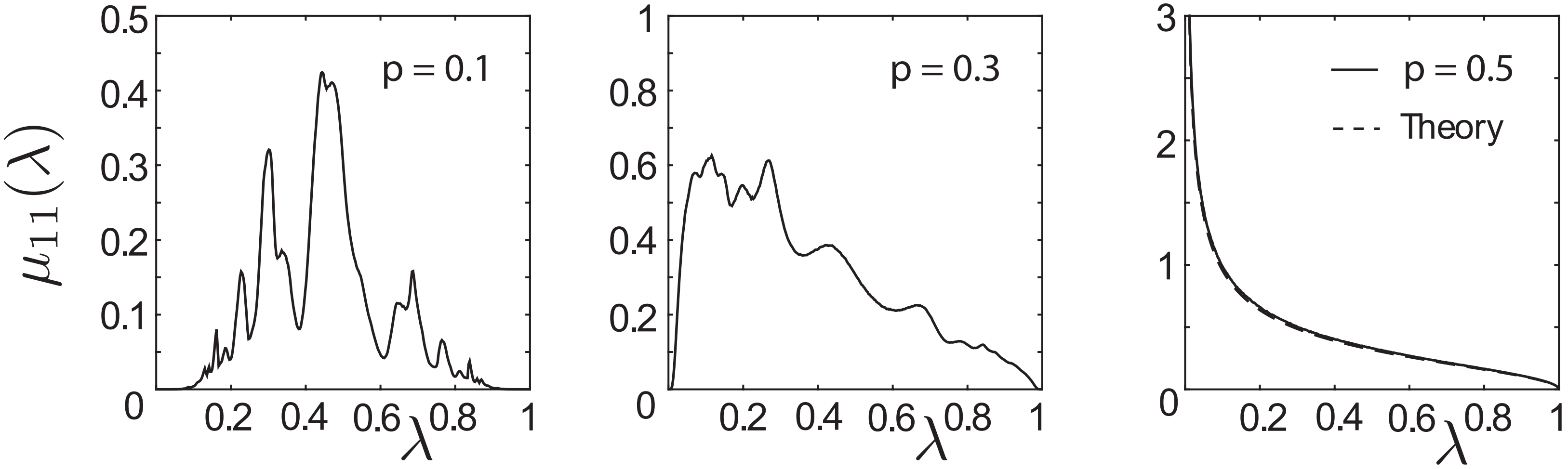

$p_c = 0.5$

Eigenvalue Spacing Distributions

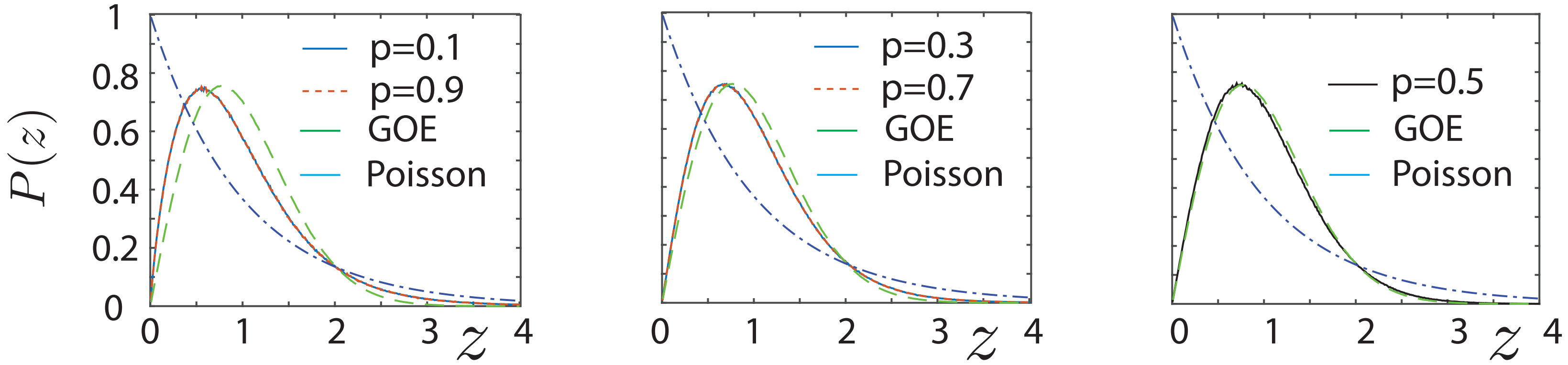

Murphy, Cherkaev, Golden, *PRL*, 2017

Eigenvalue Statistics of Random Matrix Theory

Wigner (1951) and Dyson (1953) first used random matrix theory (RMT) to describe quantized energy levels of heavy atomic nuclei.

$[\mathbf{N}]_{ij} \sim N(0,1)$, $\mathbf{A}= (\mathbf{N}+\mathbf{N}^{T})/2$ ***Gaussian orthogonal ensemble (GOE)***

$[\mathbf{N}]_{ij} \sim N(0,1)+iN(0,1)$, $\mathbf{A}= (\mathbf{N}+ \mathbf{N}^{\dagger})/2$ ***Gaussian unitary ensemble (GUE)***

Short range and long range correlations of eigenvalues are measured by various eigenvalue statistics.

Spacing distributions of energy levels for heavy atomic nuclei

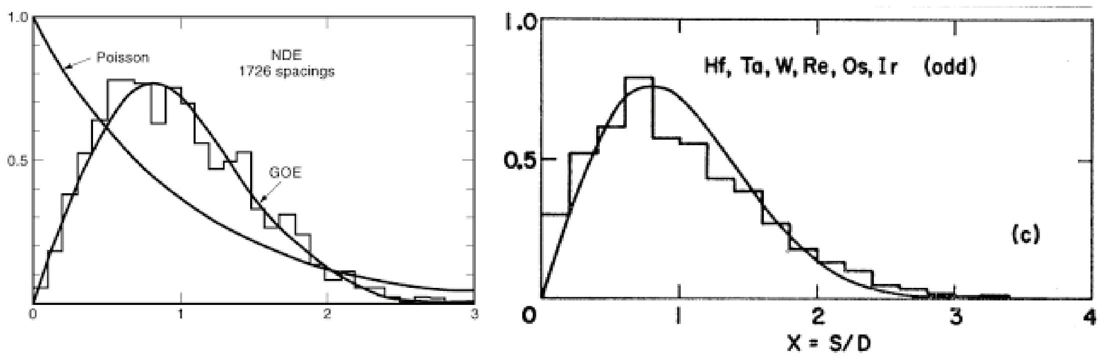

Spacing distributions of the first billion zeros of the Riemann zeta function

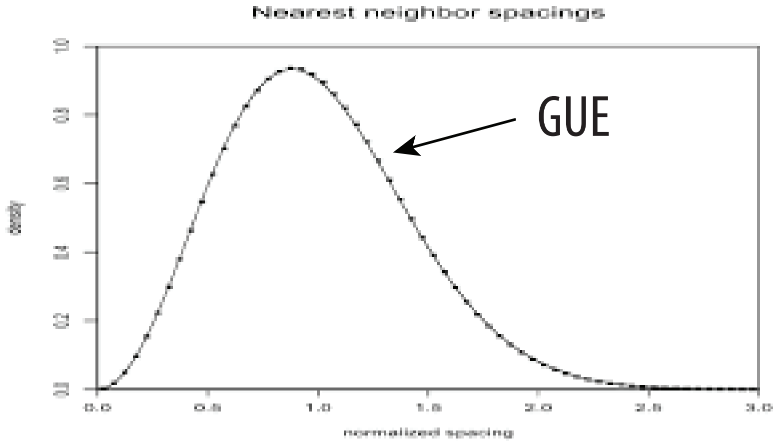

RMT used to characterize disorder-driven transitions in mesoscopic conductors, neural networks, random graph theory, etc.

Universal eigenvalue statistics arise in a broad range of "unrelated" problems!

Spectral computations for sea ice floe configurations

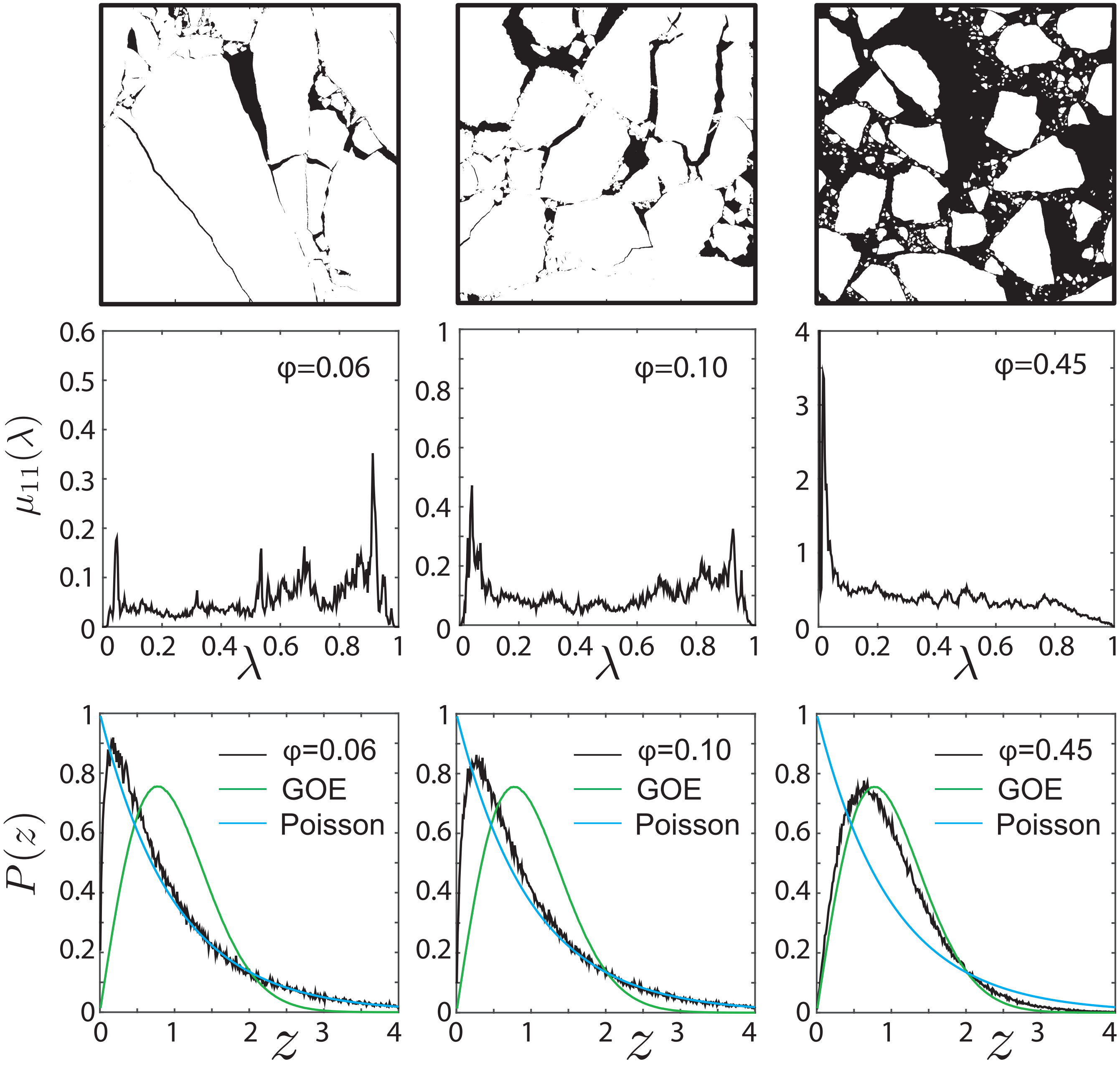

spectral measures

eigenvalue spacing distributions

UNIVERSAL Wigner-Dyson distribution

uncorrelated → **level repulsion**

ANDERSON TRANSITION

Murphy, Cherkaev, Golden
Phys. Rev. Lett. 2017

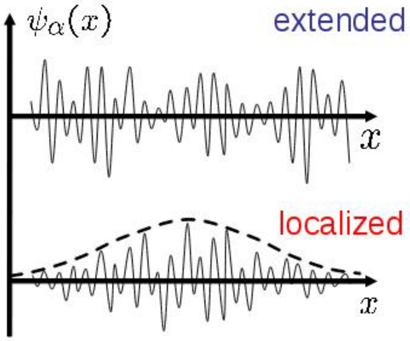

metal / insulator transition

localization

Anderson 1958
Mott 1949
Shklovshii et al 1993
Evangelou 1992

Anderson transition in wave physics:
quantum, optics, acoustics, water waves, ...

we find a surprising analog

Anderson transition for classical transport in composites

Murphy, Cherkaev, Golden Phys. Rev. Lett. 2017

PERCOLATION TRANSITION → **transition to universal eigenvalue statistics (GOE) extended states, mobility edges**

-- but without wave interference or scattering effects ! --

Homogenization for polycrystalline materials

Two-component composites

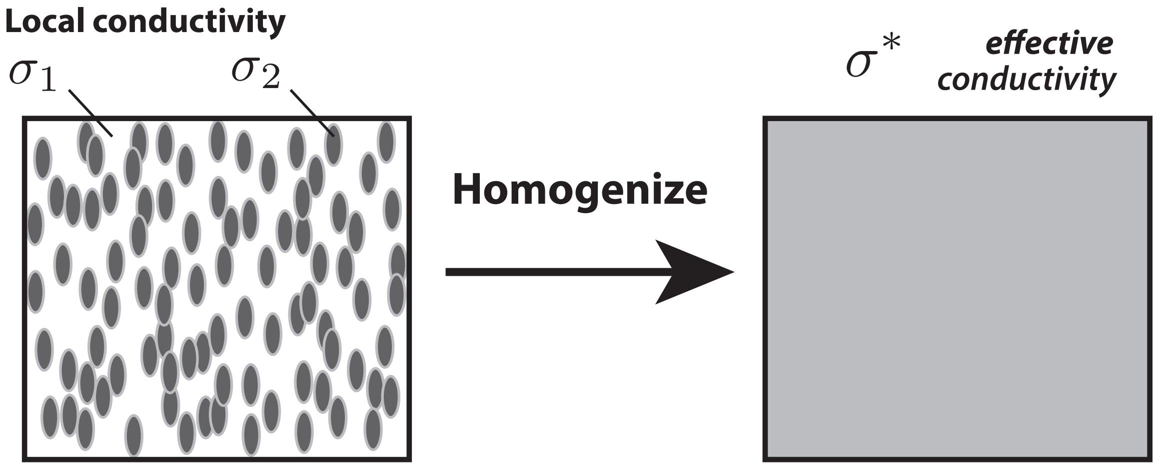

Local conductivity

σ_1 σ_2

Homogenize

σ^* ***effective conductivity***

inhomogeneous medium

homogeneous medium

Find the homogeneous medium which behaves macroscopically the same as the inhomogeneous medium

Polycrystalline media

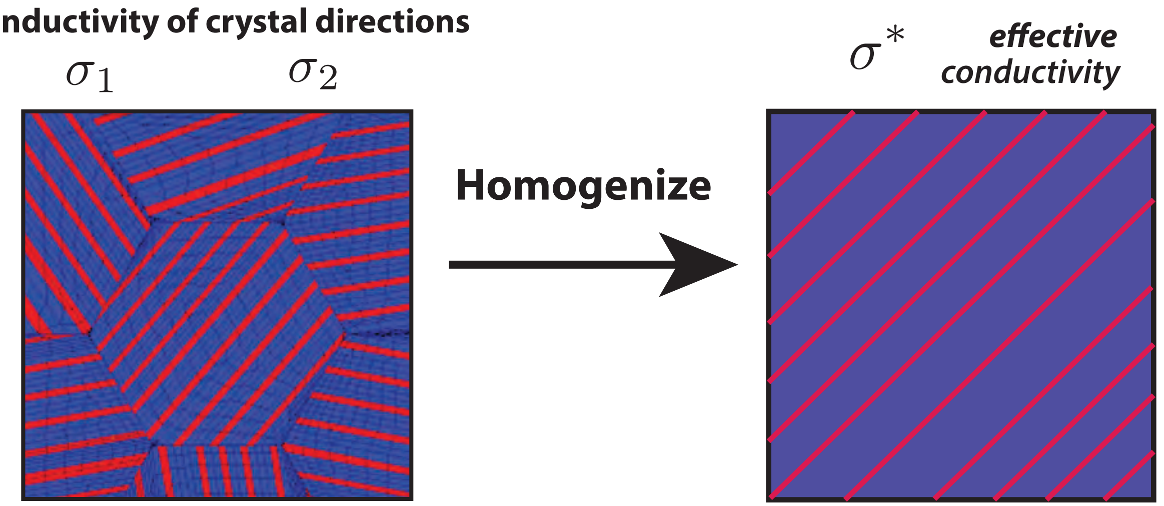

Conductivity of crystal directions

σ_1 σ_2

Homogenize

σ^* ***effective conductivity***

inhomogeneous medium

homogeneous medium

Bounds on the complex permittivity of polycrystalline materials by analytic continuation

Adam Gully, Joyce Lin,
Elena Cherkaev, Ken Golden

- **Stieltjes integral representation for effective complex permittivity**

  Milton (1981, 2002), Barabash and Stroud (1999), ...

- **Forward and inverse bounds**

  orientation statistics

- **Applied to sea ice using two-scale homogenization**

- **Inverse bounds give method for distinguishing ice types using remote sensing techniques**

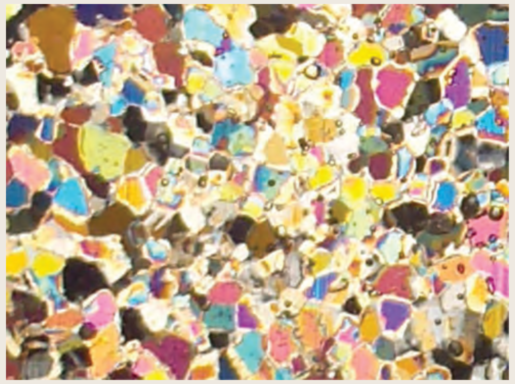

Proc. Roy. Soc. A 8 Feb 2015

Proc. R. Soc. A | Volume 471 | Issue 2174 | 8 February 2015

ISSN 1364-5021 | Volume 471 | Issue 2174 | 8 February 2015

PROCEEDINGS A

350 YEARS
OF SCIENTIFIC
PUBLISHING

An invited review commemorating 350 years of scientific publishing at the Royal Society

A method to distinguish between different types of sea ice using remote sensing techniques

A computer model to determine how a human should walk so as to expend the least energy

THE
ROYAL
SOCIETY
PUBLISHING

21/01/15 1:47 PM

higher threshold for fluid flow in Antarctic granular sea ice

columnar

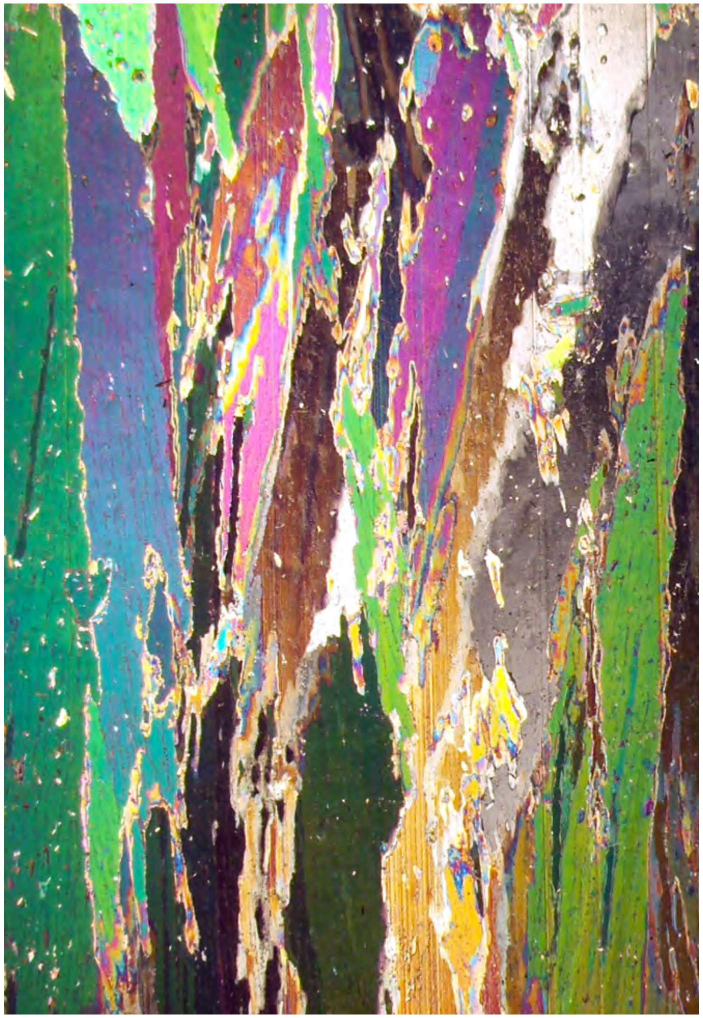

5%

granular

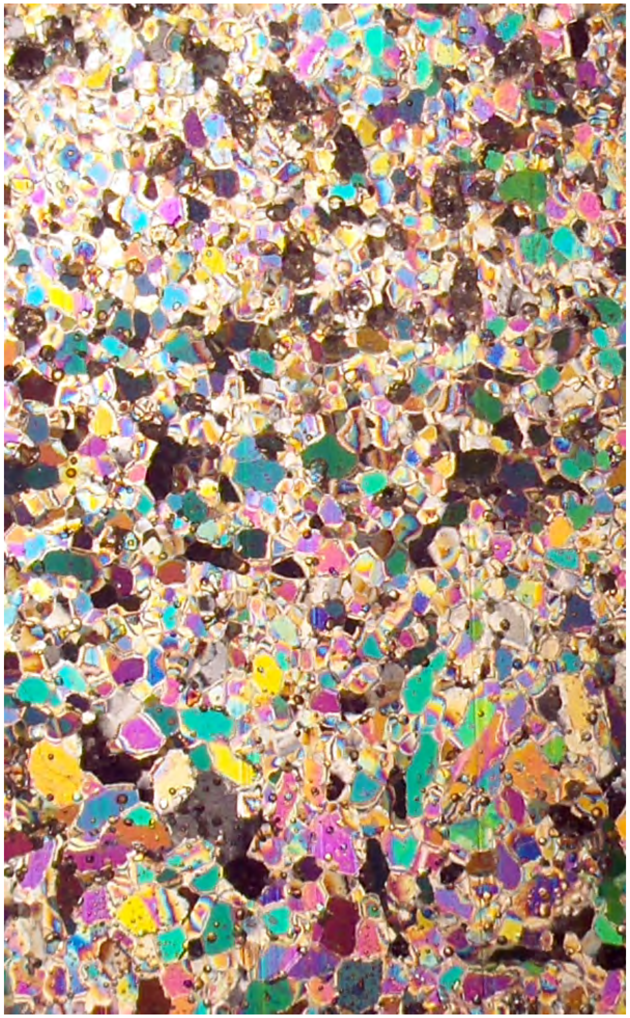

10%

Golden, Sampson, Gully, Lubbers, Tison 2020

two scale homogenization for polycrystalline sea ice

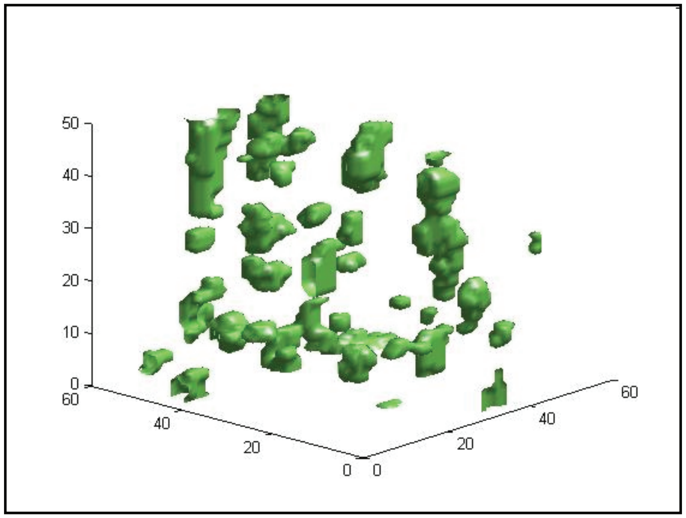

numerical homogenization for single crystal

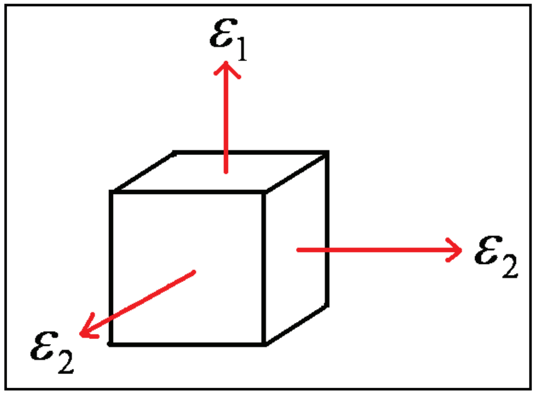

analytic continuation for polycrystals

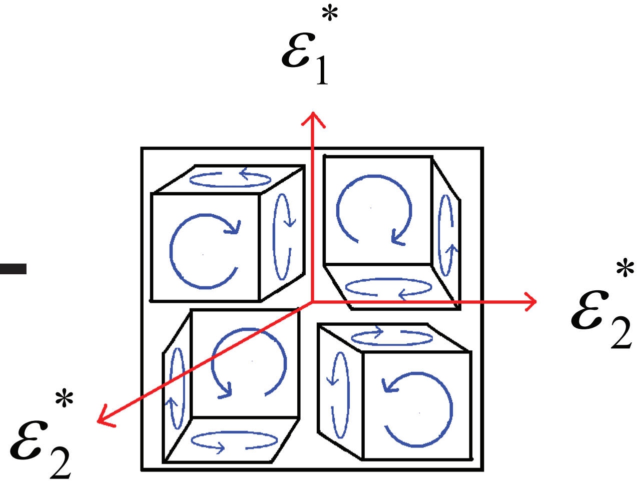

bounds

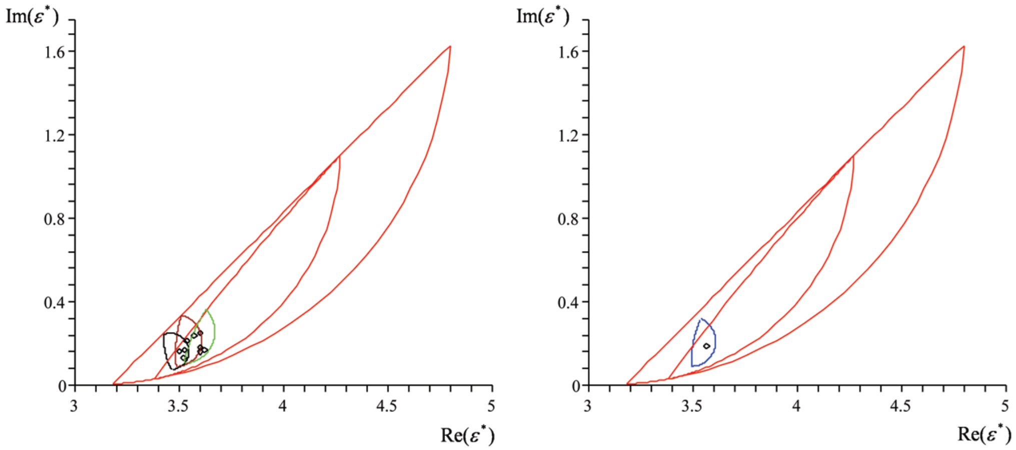

Gully, Lin, Cherkaev, Golden, Proc. Roy. Soc. A (and cover) 2015

Rigorous bounds on the complex permittivity tensor of sea ice with polycrystalline anisotropy within the horizontal plane

McKenzie McLean, Elena Cherkaev, Ken Golden 2020

motivated by **Weeks and Gow, *JGR* 1979: c-axis alignment in Arctic fast ice off Barrow**

Golden and Ackley, *JGR* 1981: radar propagation model in aligned sea ice

input: orientation statistics

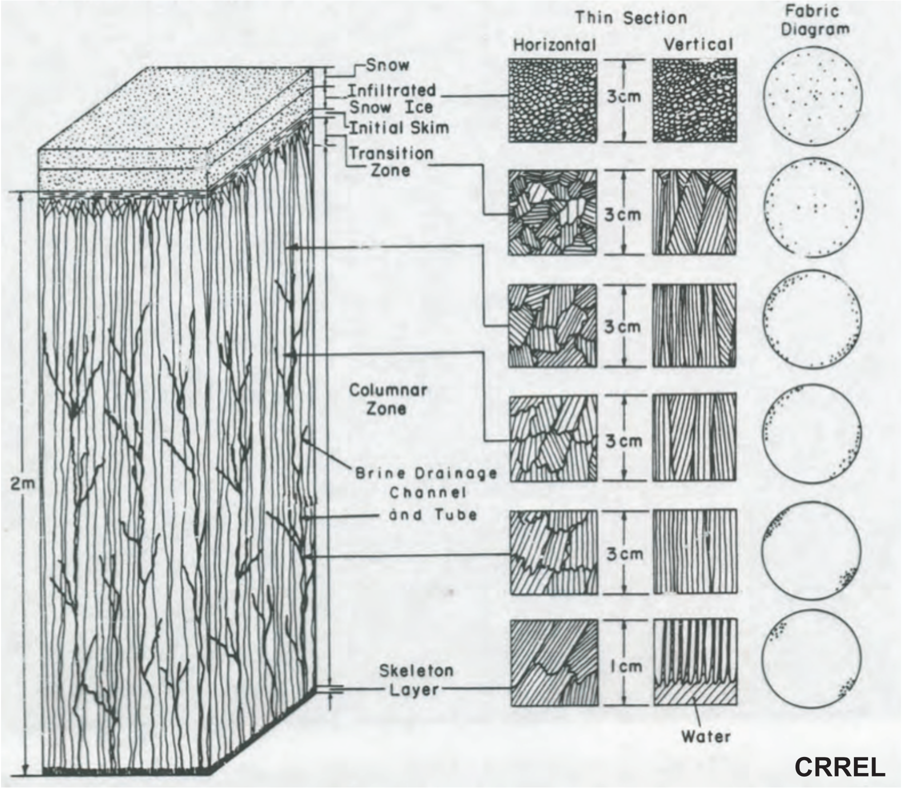

output: bounds

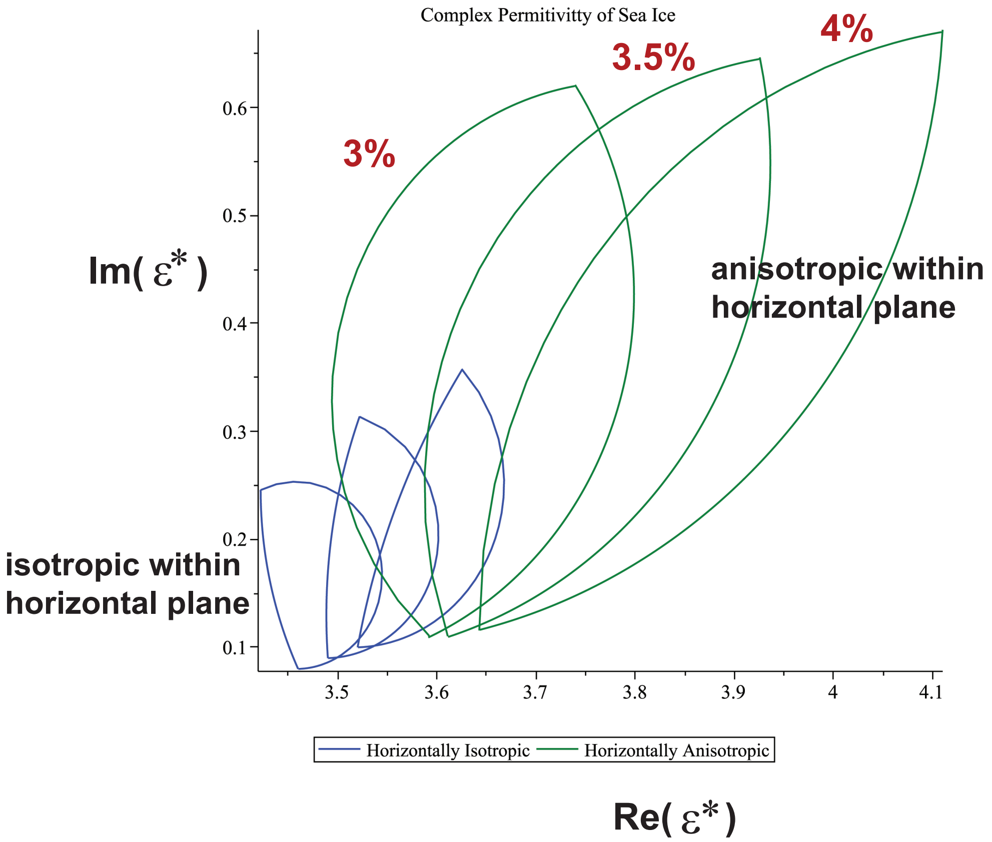

wave propagation in the marginal ice zone

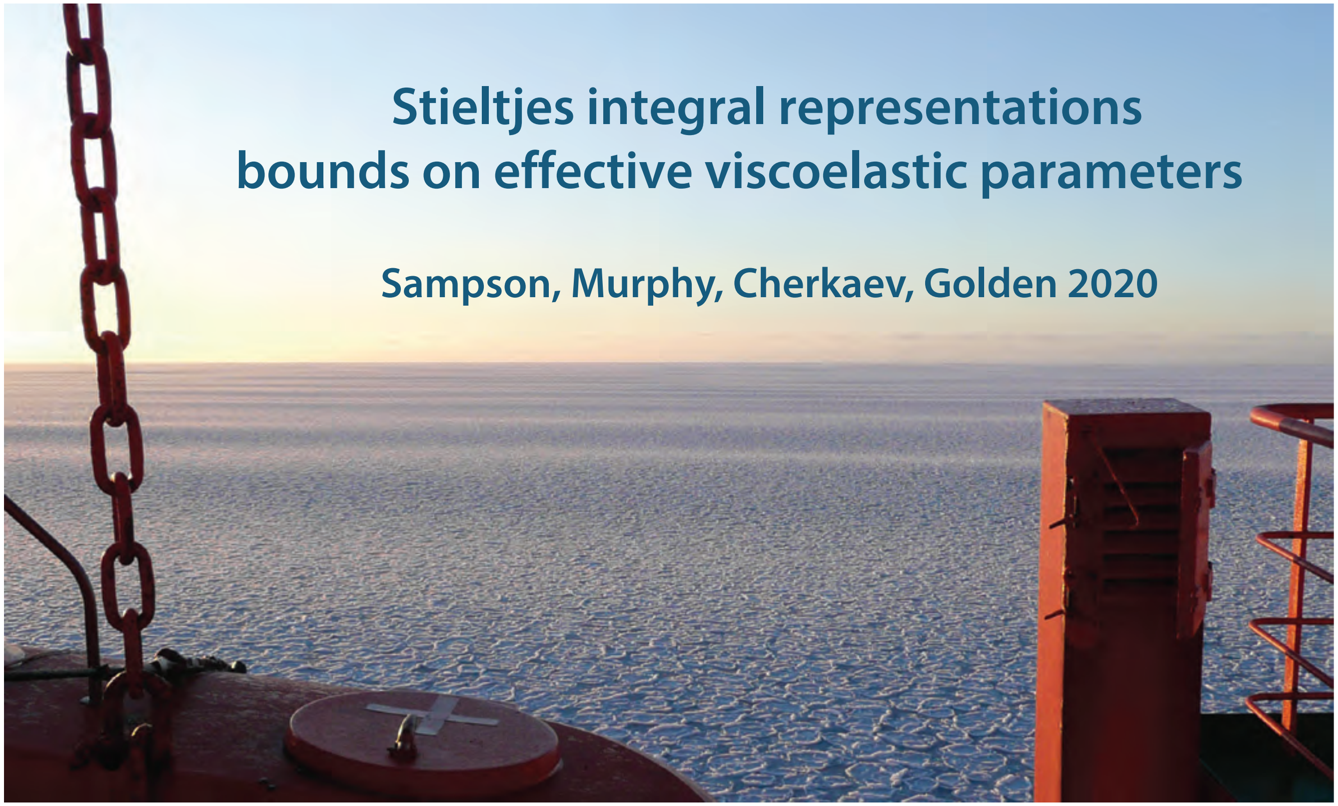

Stieltjes integral representations
bounds on effective viscoelastic parameters

Sampson, Murphy, Cherkaev, Golden 2020

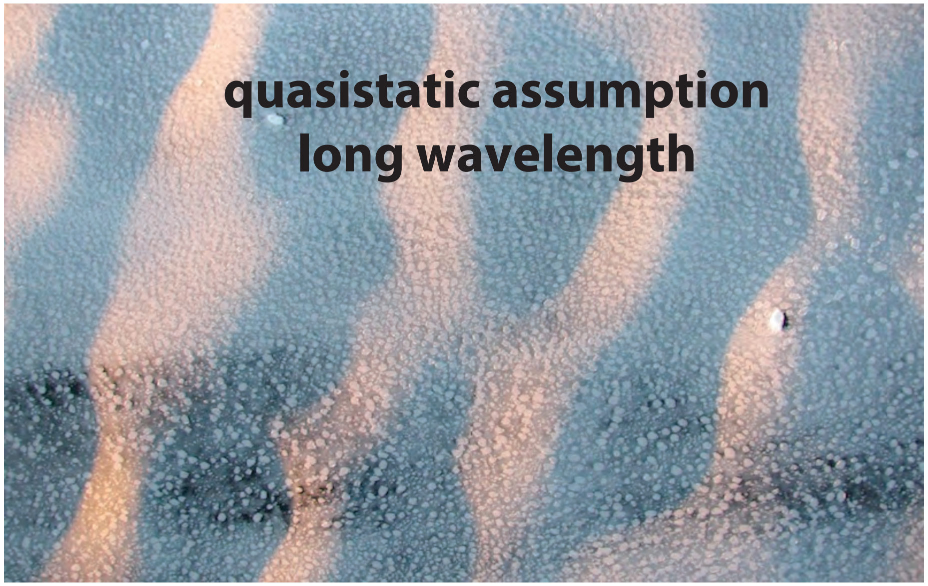

quasistatic assumption
long wavelength

bounds on the effective complex viscoelasticity

complex elementary bounds
(fixed area fraction of floes)

$\nu_1 = 10^7 + i\,4875$ **pancake ice**

$\nu_2 = 5 + i\,0.0975$ **slush / frazil**

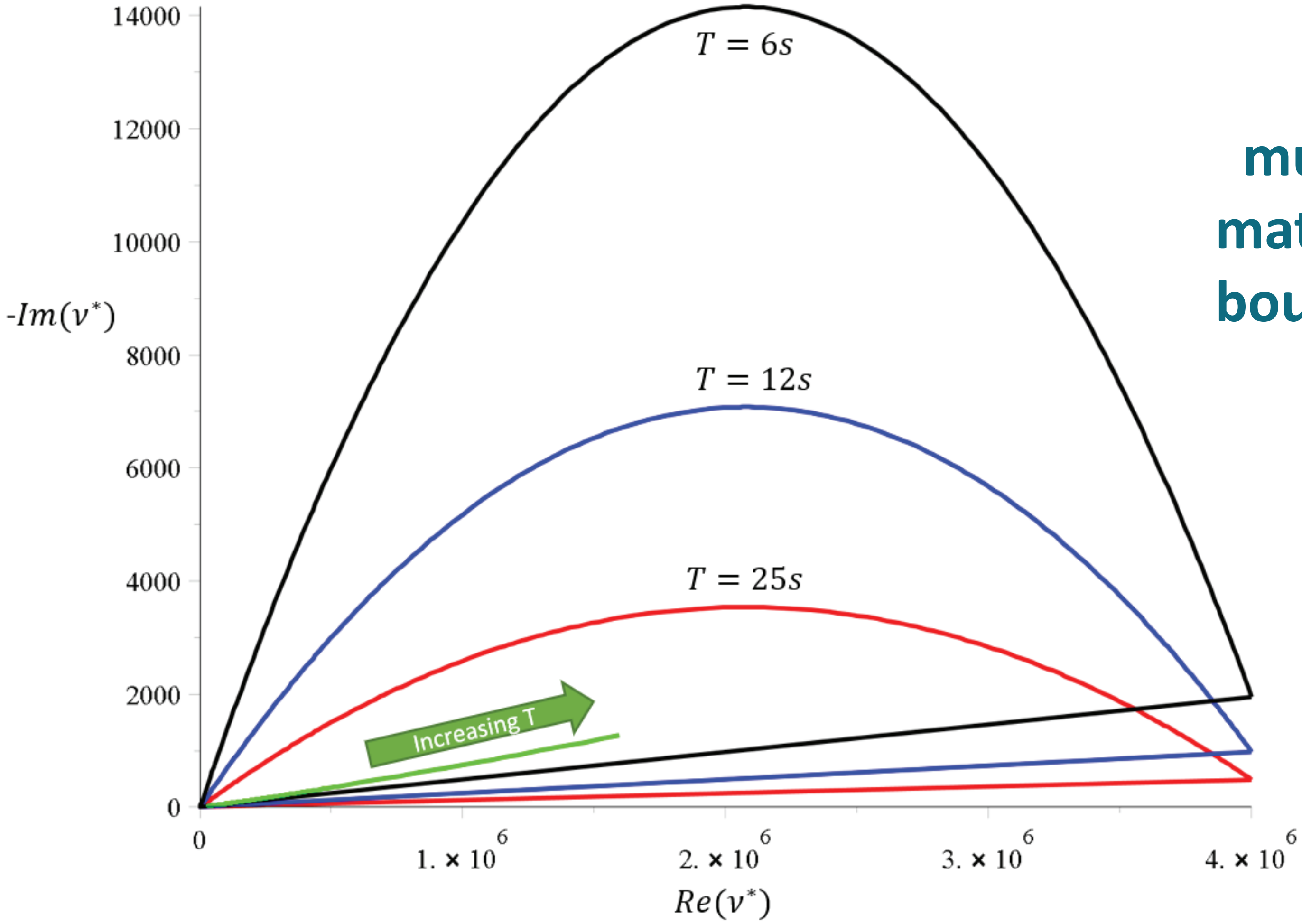

+
much tighter
matrix particle
bounds + data

Sampson, Murphy, Cherkaev, Golden 2020

advection enhanced diffusion

effective diffusivity

nutrient and salt transport in sea ice
heat transport in sea ice with convection
sea ice floes in winds and ocean currents
tracers, buoys diffusing in ocean eddies
diffusion of pollutants in atmosphere

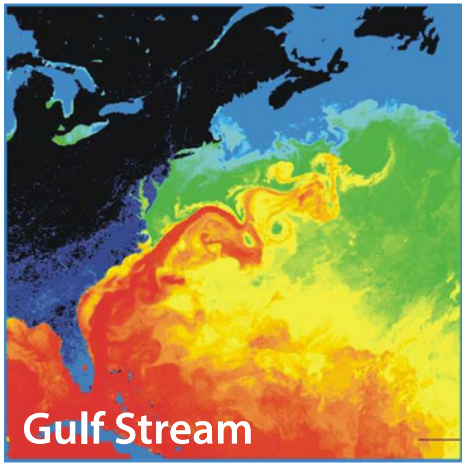

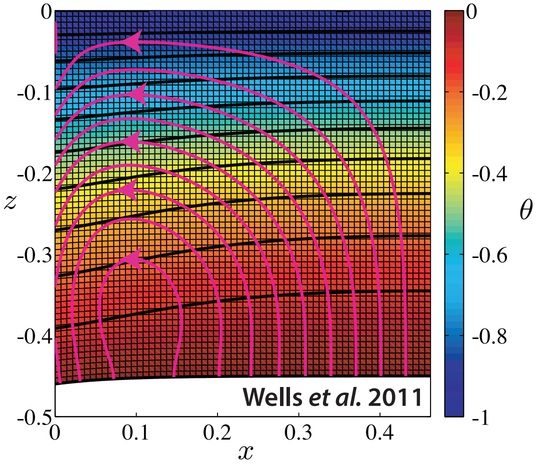

advection diffusion equation with a velocity field $\vec{u}$

$$\frac{\partial T}{\partial t} + \vec{u} \cdot \vec{\nabla} T = \kappa_0 \Delta T$$

$$\vec{\nabla} \cdot \vec{u} = 0$$

homogenize

$$\frac{\partial \overline{T}}{\partial t} = \kappa^* \Delta \overline{T}$$

κ^* ***effective diffusivity***

Stieltjes integral for κ^* ***with spectral measure***

Avellaneda and Majda, PRL 89, CMP 91

Murphy, Cherkaev, Xin, Zhu, Golden, *Ann. Math. Sci. Appl.* 2017
Murphy, Cherkaev, Zhu, Xin, Golden, *J. Math. Phys.* 2020

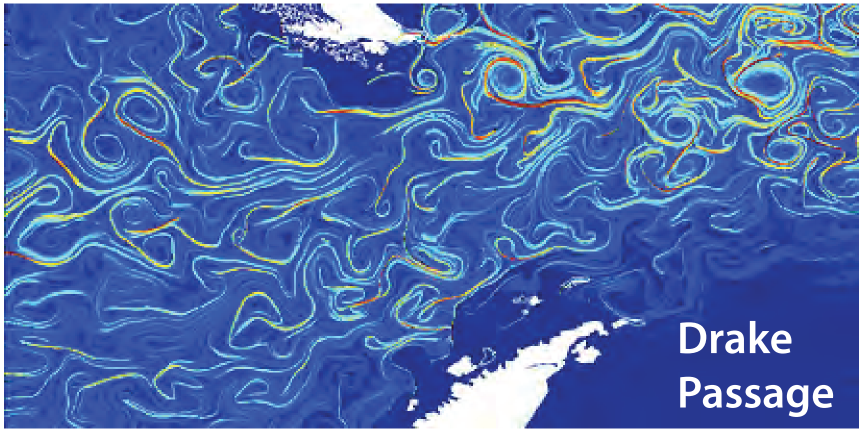

tracers flowing through inverted sea ice blocks

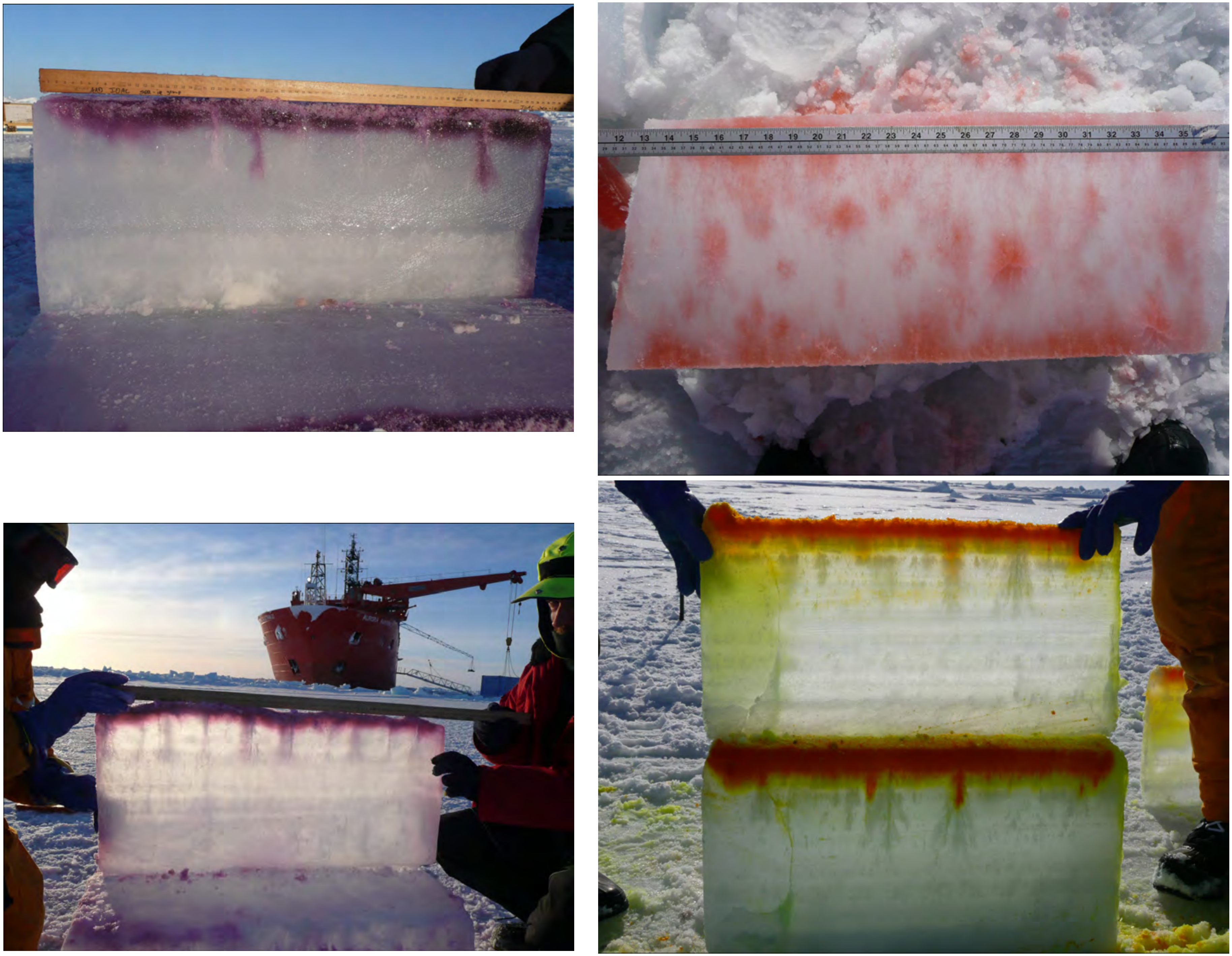

Stieltjes integral for κ^* with spectral measure

composites

Golden and Papanicolaou, CMP 1983

$$\frac{\epsilon^*}{\epsilon_2} = 1 - \int_0^1 \frac{d\mu(\lambda)}{s-\lambda}$$

$$s = \frac{1}{1 - \epsilon_1 / \epsilon_2}$$

advection diffusion

Avellaneda and Majda, PRL 89, CMP 91

$$\frac{\kappa^*}{\kappa} = 1 - \int_0^\infty \frac{d\rho(z)}{t-z}$$

$t = -1/\xi^2, \ \ \xi$ = Péclet number

- computations of spectral measures and effective diffusivity for model flows; new representations, moment calculations

Murphy, Cherkaev, Zhu, Xin, Golden, *J. Math. Phys.* 2020

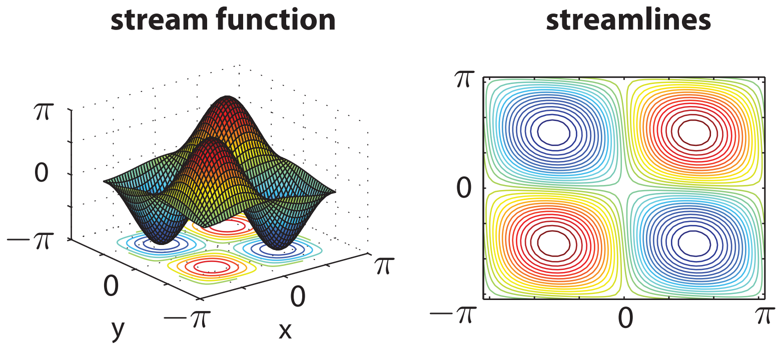
stream function

streamlines

- rigorous bounds and computations for convection enhanced thermal conductivity of sea ice

Kraitzman, Hardenbrook, Dinh, Murphy, Zhu, Cherkaev, Golden 2020

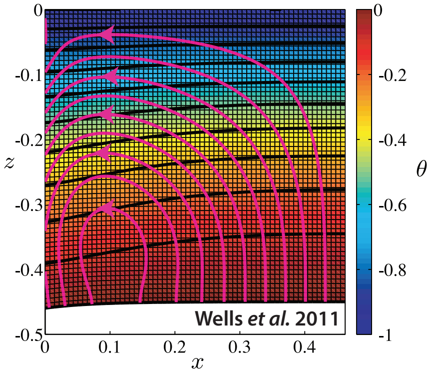
Wells *et al.* 2011

Stieltjes Integral Representation for Advection Diffusion

Murphy, Cherkaev, Zhu, Xin, Golden, *J. Math. Phys.* 2020

$$\kappa^* = \kappa \left(1 + \int_{-\infty}^{\infty} \frac{d\mu(\tau)}{\kappa^2 + \tau^2} \right), \quad F(\kappa) \ = \int_{-\infty}^{\infty} \frac{d\mu(\tau)}{\kappa^2 + \tau^2}$$

- μ is a positive definite measure corresponding to the spectral resolution of the self-adjoint operator $i\Gamma H \Gamma$
- $H =$ stream matrix , $\kappa =$ local diffusivity
- $\Gamma := -\nabla(-\Delta)^{-1}\nabla\cdot$, Δ is the Laplace operator
- $i\Gamma H \Gamma$ is bounded for time independent flows
- $F(\kappa)$ is analytic off the spectral interval in the κ-plane

separation of material properties and flow field

spectral measure calculations

Rigorous bounds on convection enhanced thermal conductivity of sea ice

Kraitzman, Hardenbrook, Dinh, Murphy, Zhu, Cherkaev, Golden 2020

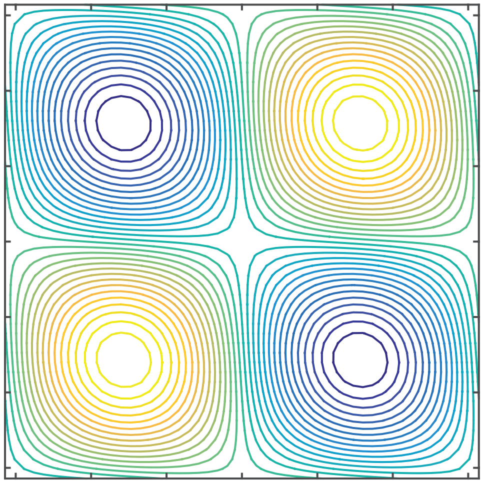

cat's eye flow model for
brine convection cells

similar bounds
for shear flows

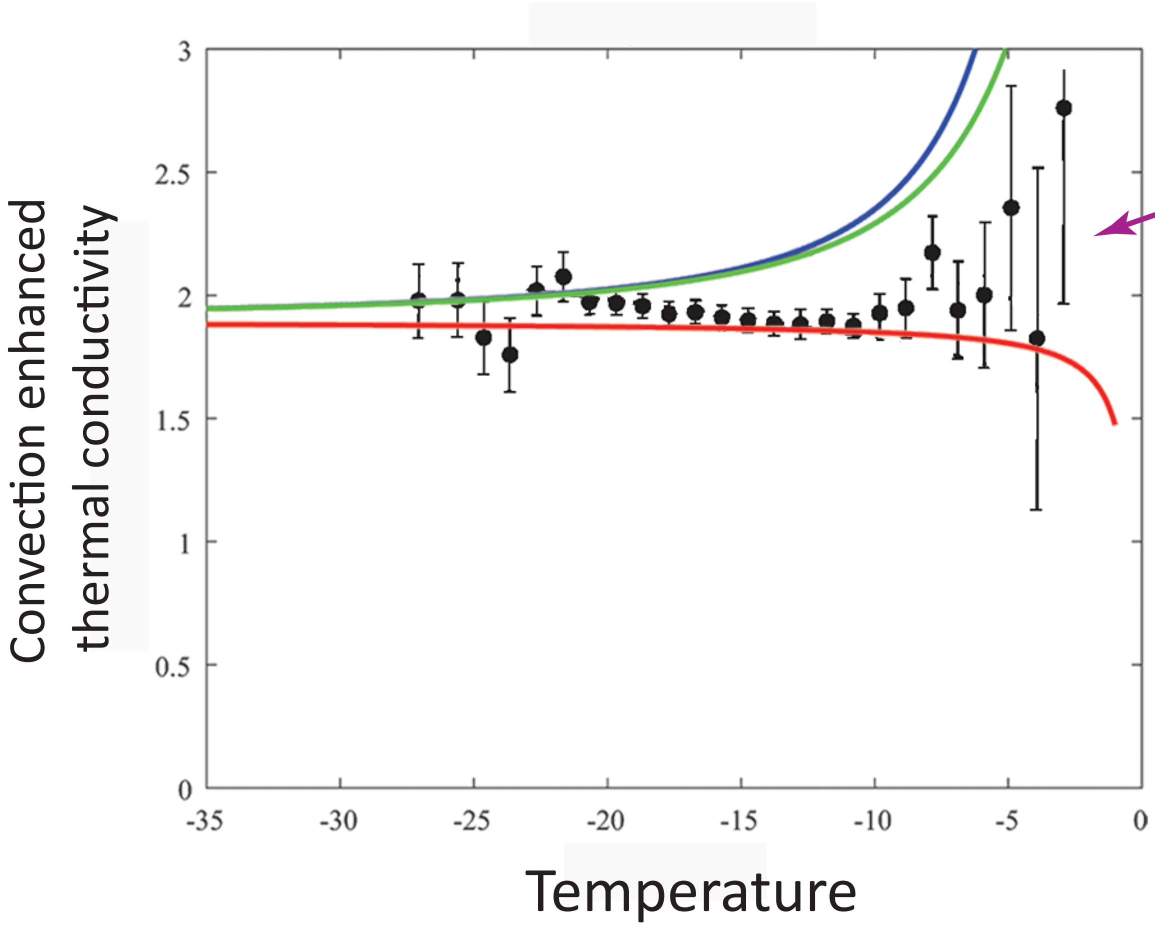

data
Trodahl
et al. 2001

rigorous Padé bounds from Stieltjes integral +
analytical calculations of moments of measure

rigorous bounds assuming information
on flow field INSIDE inclusions

Kraitzman, Cherkaev, Golden
in revision, 2020

Anomalous diffusion in sea ice dynamics

Ice floe diffusion in winds and currents

Jennifer Lukovich, Jennifer Hutchings,
David Barber, *Ann. Glac.* 2015

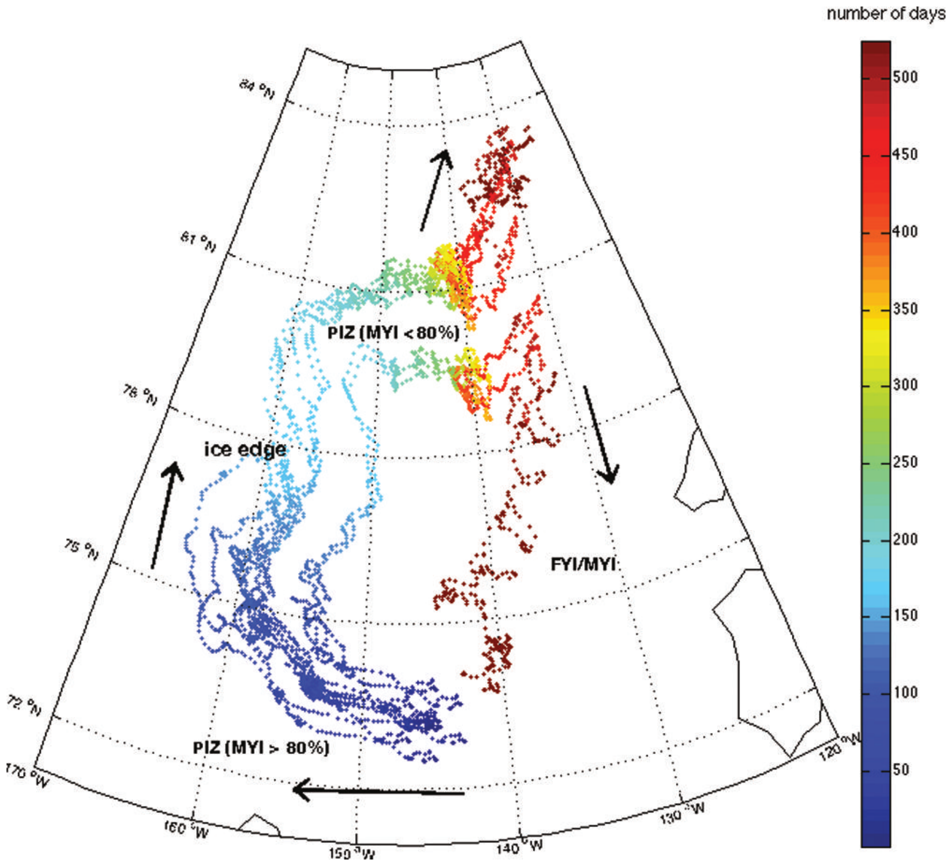

- **On short time scales floes observed (buoy data) to exhibit Brownian-like behavior, but they are also being advected by winds and currents.**

- **Effective behavior is purely diffusive, sub-diffusive or super-diffusive depending on ice pack and advective conditions - Hurst exponent.**

Floe Scale Model of Anomalous Diffusion in Sea Ice Dynamics

Huy Dinh, Elena Cherkaev, Court Strong, Ken Golden 2020

$$\left\langle \left| \mathbf{x}(t) - \mathbf{x}(0) - \langle \mathbf{x}(t) - \mathbf{x}(0) \rangle \right|^2 \right\rangle \sim t^\alpha$$

$\alpha =$ Hurst exponent, a measure of anomalous diffusion.

Measured from bouy position data. Detects ice pack crowding and advective forcing.

J.V. Lukovich, J.K. Hutchings, D.G. Barber *Annals of Glaciology* **2015**

diffusive	$\alpha = 1$	Sparse packing, uncorrelated advective field.
sub-diffusive	$\alpha < 1$	Dense packing, crowding dominates advection.
super-diffusive	$\alpha = 5/4$	Sparse packing, shear dominates advection.
	$\alpha = 5/3$	Sparse packing, vorticity dominates advection.

Goal: Develop numerical model to analyze regimes of transport in terms of ice pack crowding and advective conditions.

Model Results

Crowding in random advective forcing.

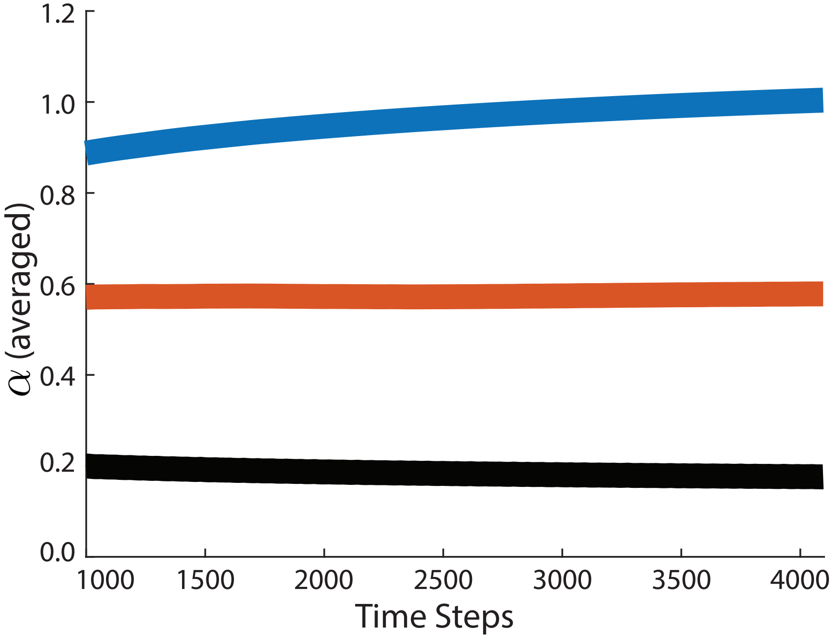

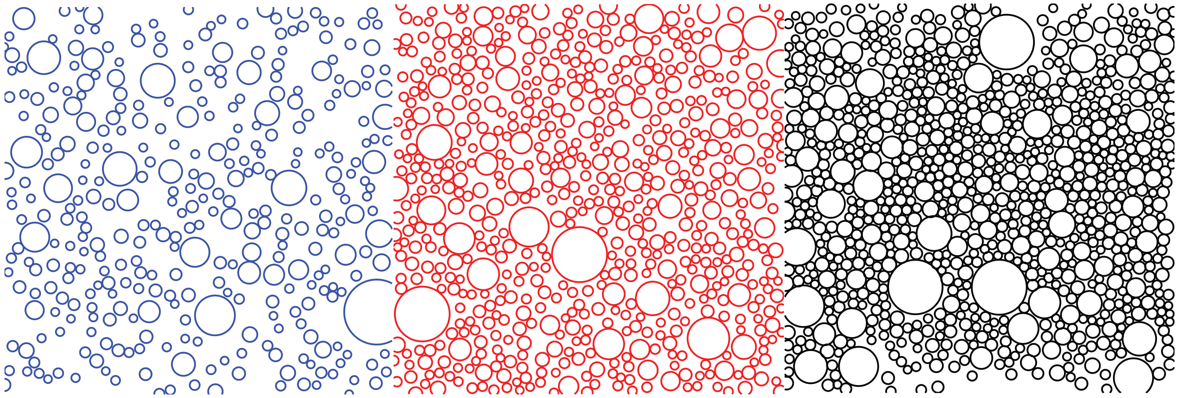

Concentration = 0.3
k = 2.9

Concentration = 0.5
k = 2.9

Concentration = 0.7
k = 2.9

$\alpha = 5/3$

Concentration = 0.3 k = 2.9

Vorticity Dominated Drift

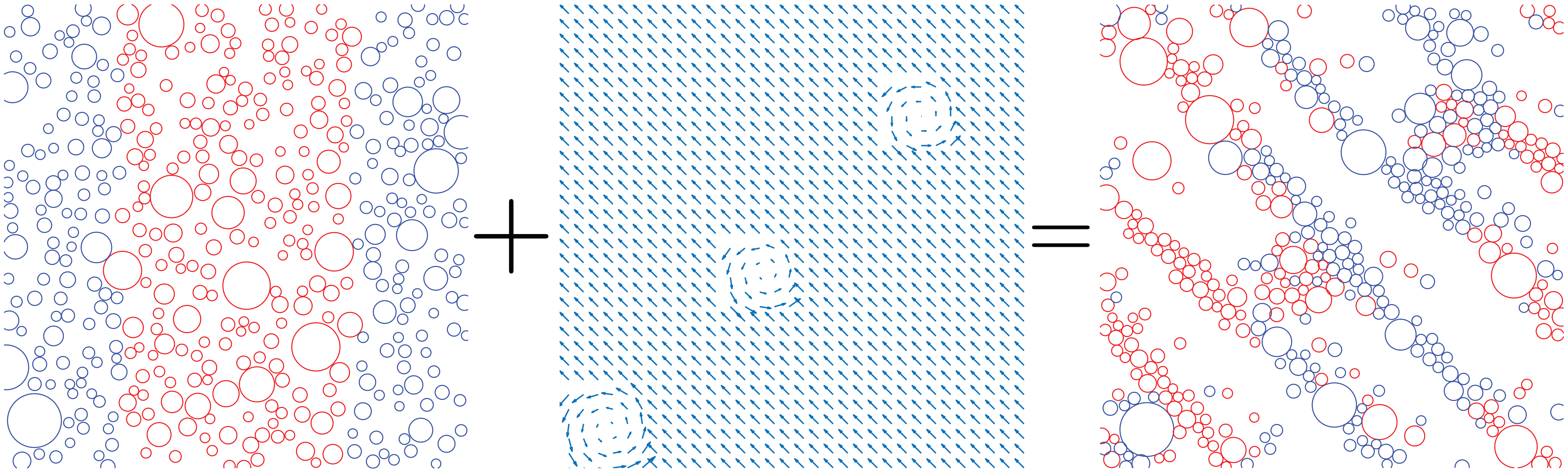

Marginal Ice Zone

MIZ

- biologically active region
- intense ocean-sea ice-atmosphere interactions
- region of significant wave-ice interactions

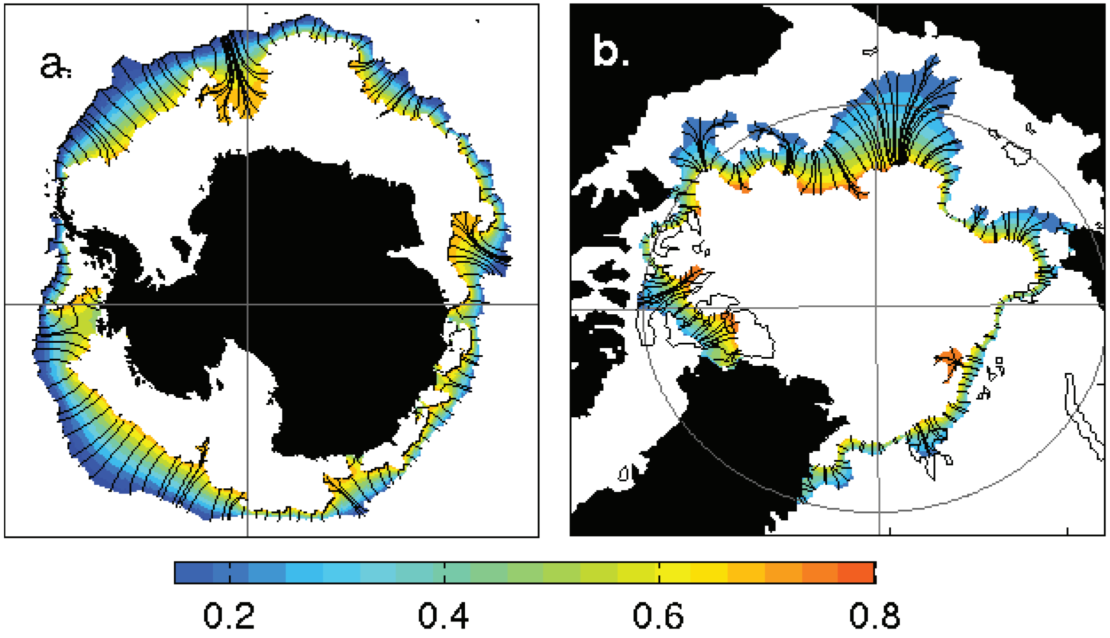

transitional region between dense interior pack ($c > 80\%$) sparse outer fringes ($c < 15\%$)

MIZ WIDTH

fundamental length scale of ecological and climate dynamics

Strong, *Climate Dynamics* 2012
Strong and Rigor, *GRL* 2013

How to objectively measure the "width" of this complex, non-convex region?

Objective method for measuring MIZ width motivated by medical imaging and diagnostics

Strong, *Climate Dynamics* 2012
Strong and Rigor, *GRL* 2013

39% widening
1979 - 2012

"average" lengths of streamlines

streamlines of a solution to Laplace's equation

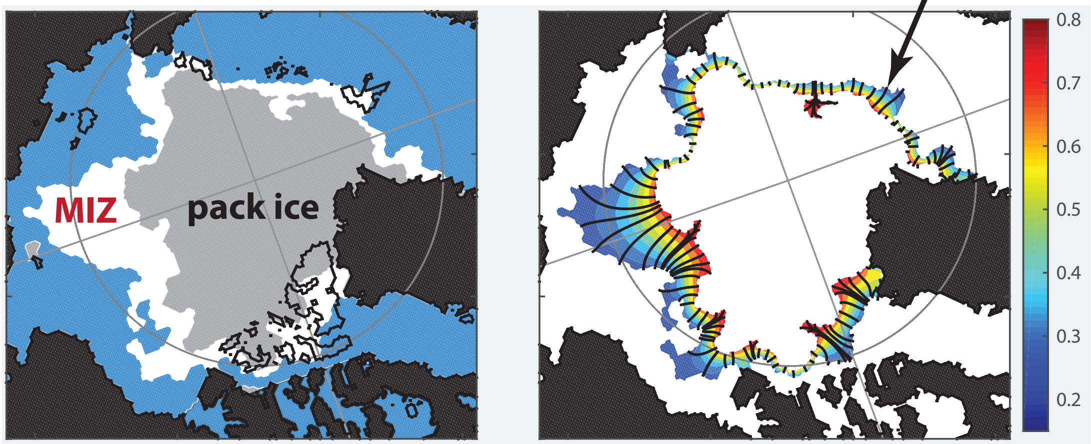

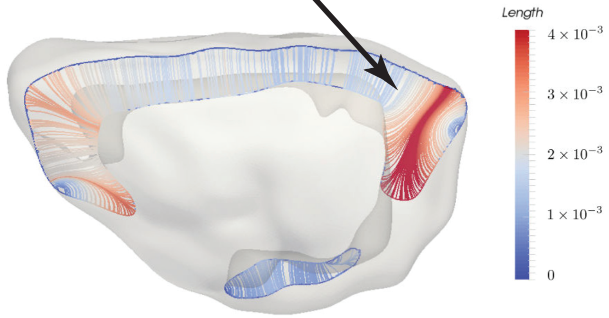

Arctic Marginal Ice Zone

crossection of the cerebral cortex of a rodent brain

analysis of different MIZ WIDTH definitions

Strong, Foster, Cherkaev, Eisenman, Golden
J. Atmos. Oceanic Tech. 2017

Strong and Golden
Society for Industrial and Applied Mathematics News, April 2017

Filling the polar data gap

hole in satellite coverage of sea ice concentration field

previously assumed ice covered

Gap radius: 611 km
06 January 1985

Gap radius: 311 km
30 August 2007

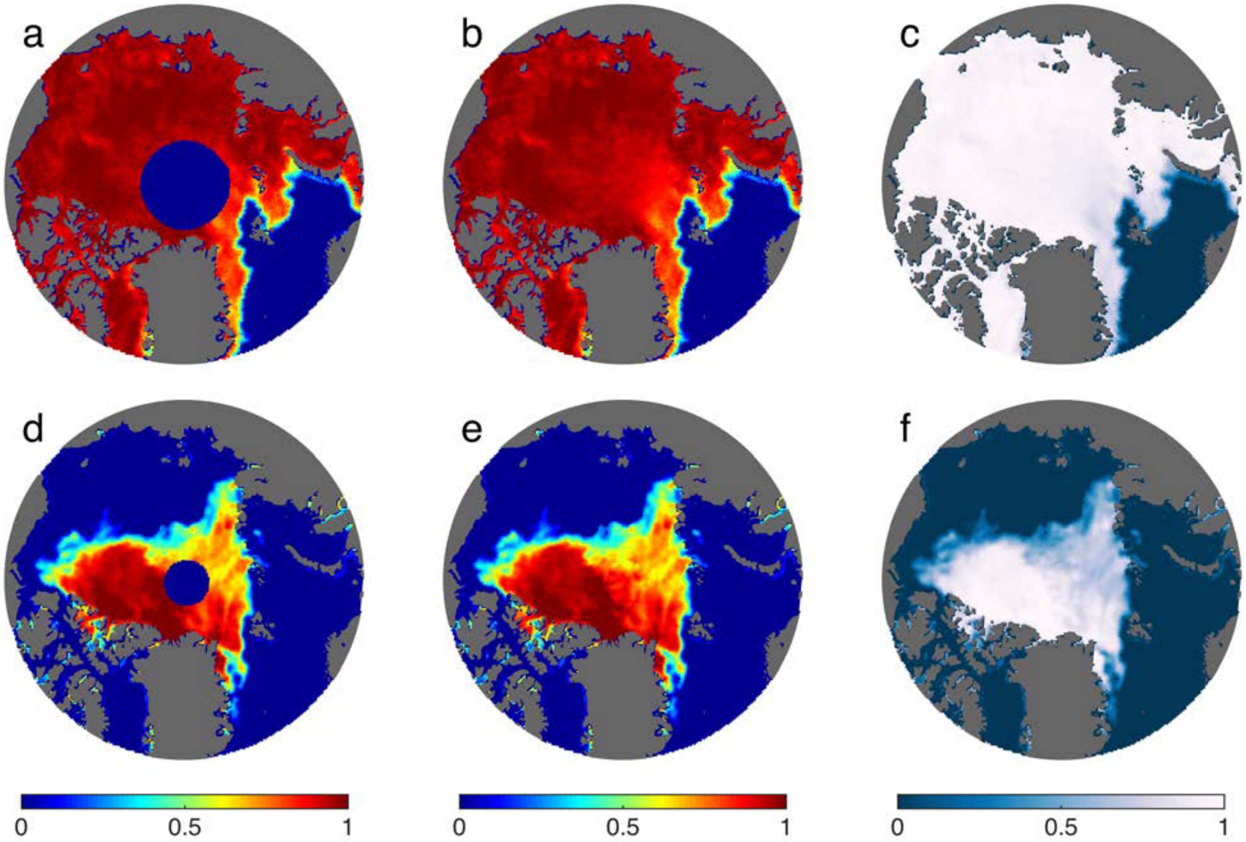

fill with harmonic function satisfying satellite BC's plus stochastic term

Strong and Golden, *Remote Sensing* 2016
Strong and Golden, *SIAM News* 2017

melt pond formation and albedo evolution:

- *major drivers in polar climate*
- *key challenge for global climate models*

numerical models of melt pond evolution, including topography, drainage (permeability), etc.

Lüthje, Feltham, Taylor, Worster 2006

Flocco, Feltham 2007

Skyllingstad, Paulson, Perovich 2009

Flocco, Feltham, Hunke 2012

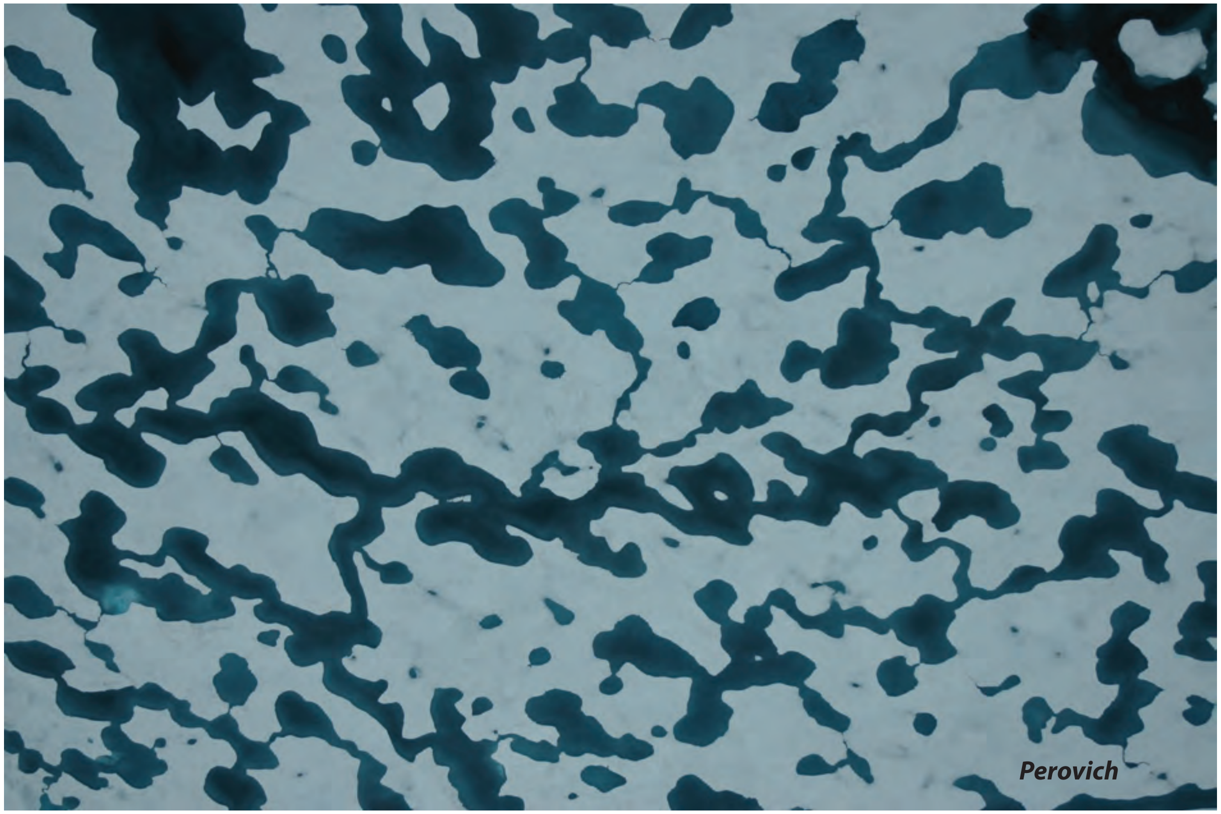

Are there universal features of the evolution similar to phase transitions in statistical physics?

fractal curves in the plane

they wiggle so much that their dimension is >1

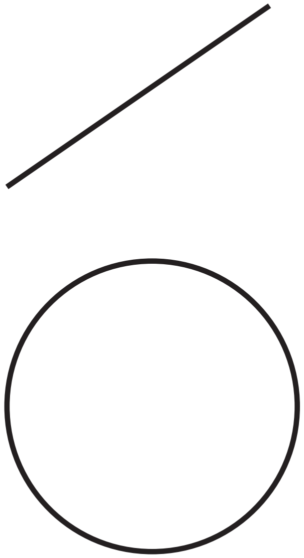

simple curves

D = 1

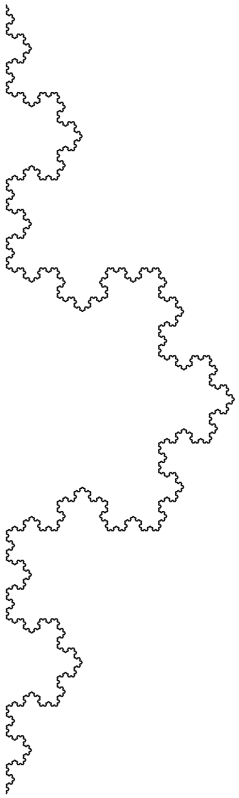

Koch snowflake

D = 1.26

Peano curve

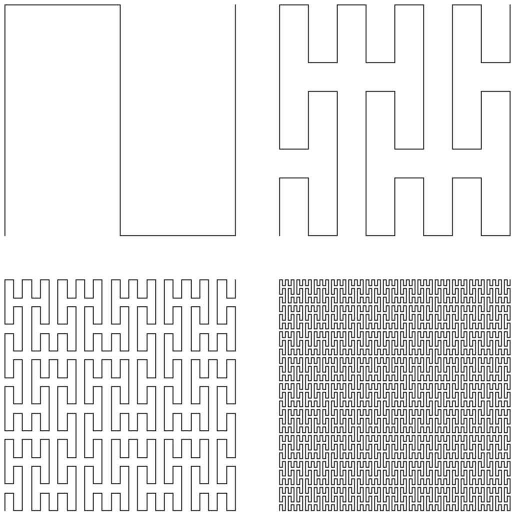

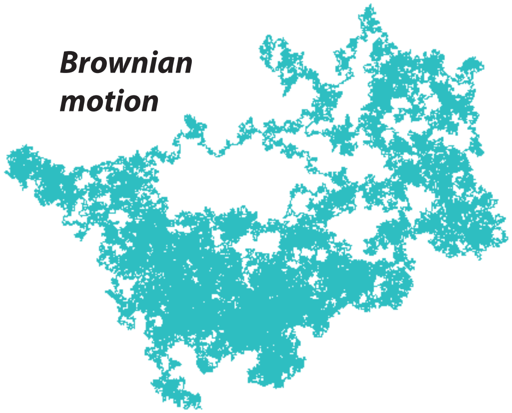

Brownian motion

space filling curves

D = 2

Transition in the fractal geometry of Arctic melt ponds

Christel Hohenegger, Bacim Alali, Kyle Steffen, Don Perovich, Ken Golden

The Cryosphere, 2012

complexity grows with length scale

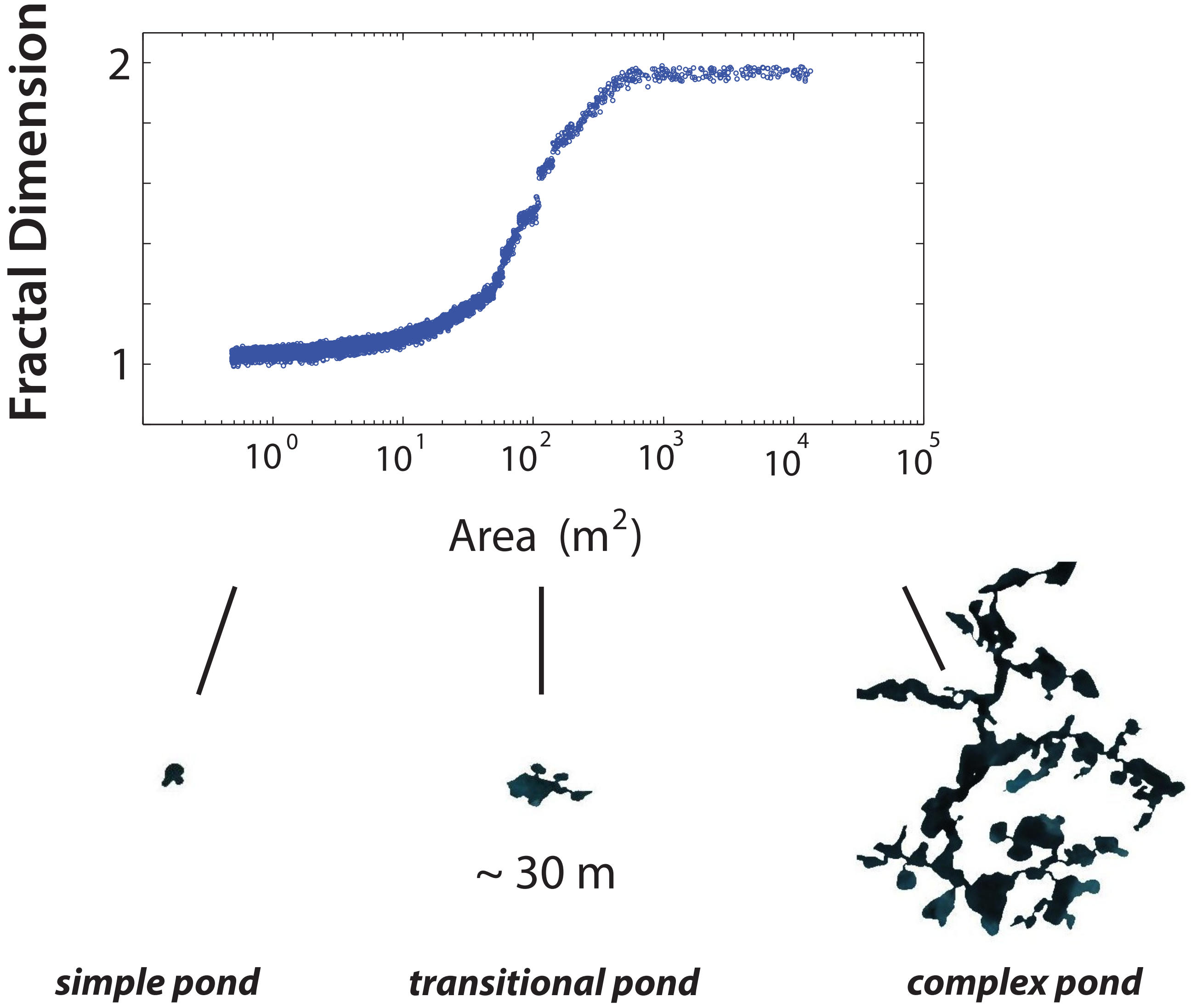

Continuum percolation model for melt pond evolution

level sets of random surfaces

Brady Bowen, Court Strong, Ken Golden, J. Fractal Geometry 2018

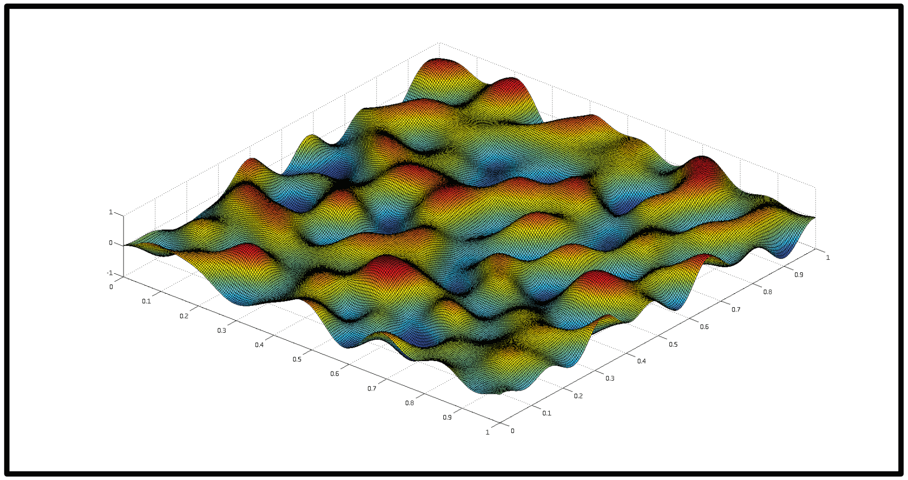

random Fourier series representation of surface topography

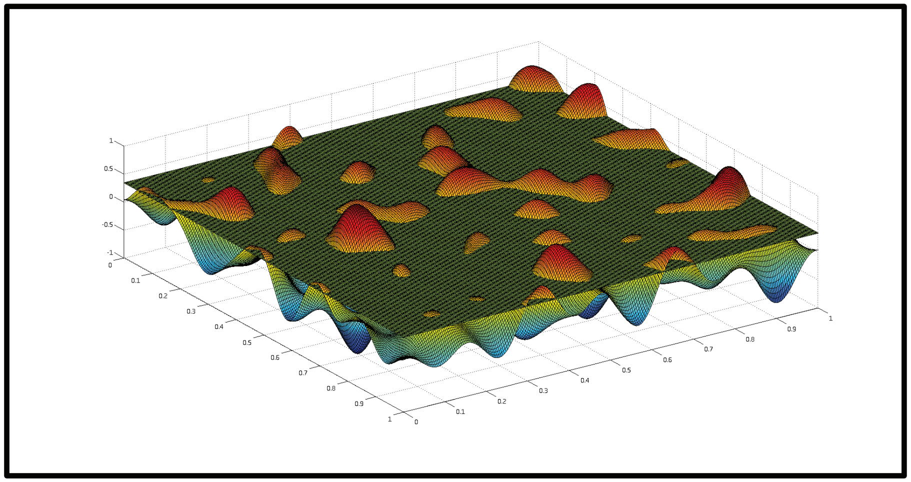

intersections of a plane with the surface define melt ponds

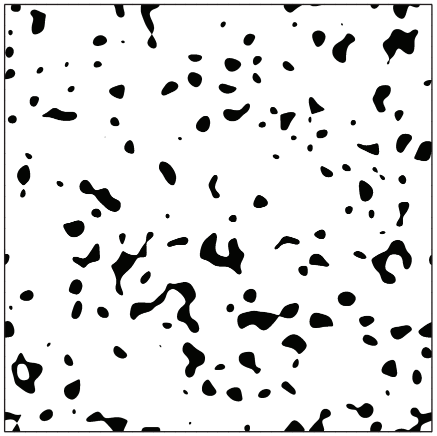

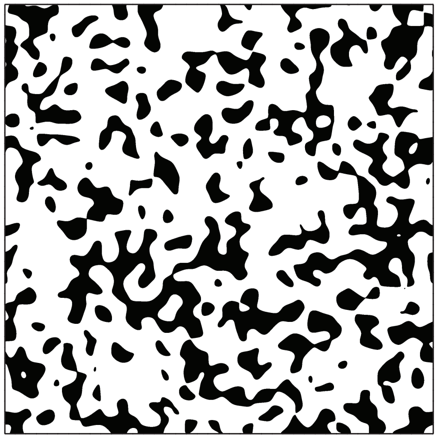

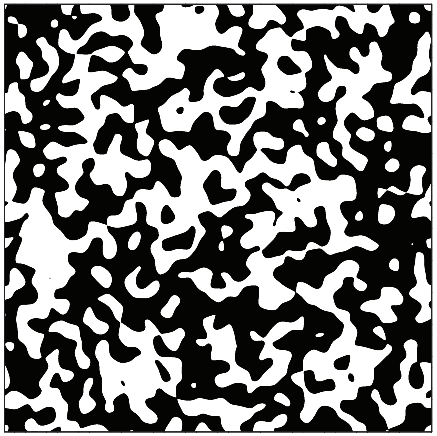

electronic transport in disordered media

diffusion in turbulent plasmas

Isichenko, Rev. Mod. Phys., 1992

fractal dimension curves depend on statistical parameters defining random surface

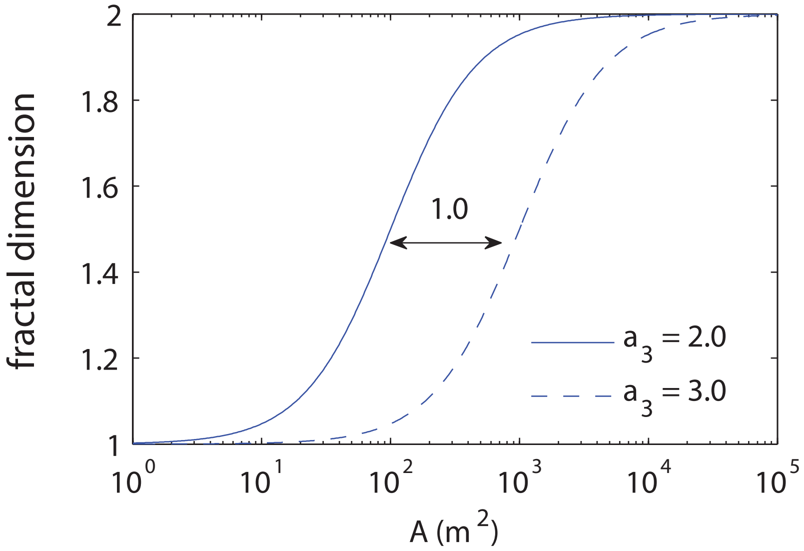

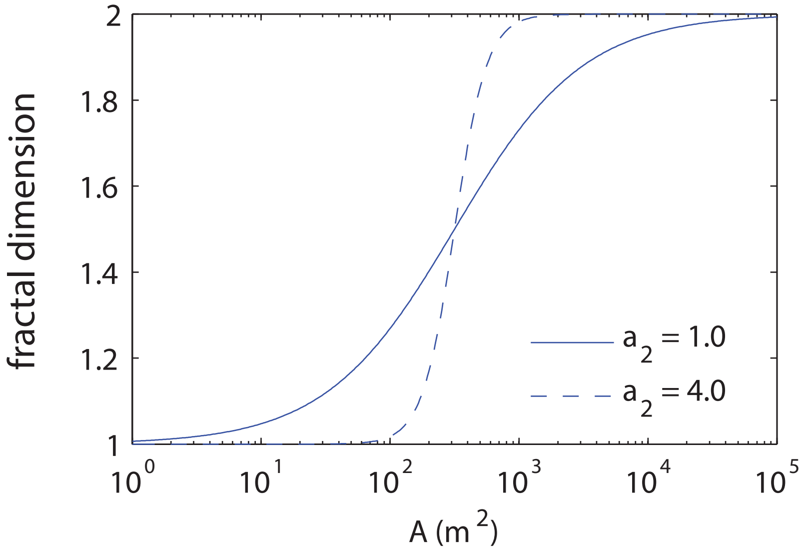

Saddle Points: The Key to Melt Pond Evolution

Ryleigh Moore, Jacob Jones, Dane Gollero, Court Strong, Ken Golden 2020

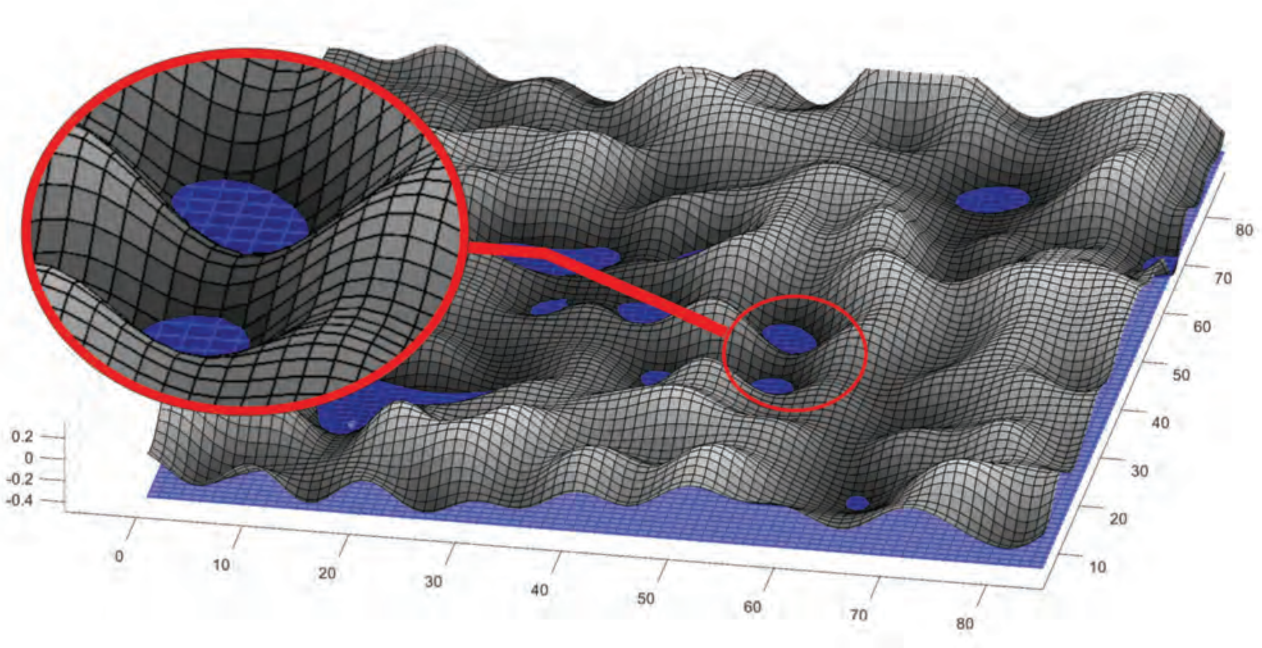

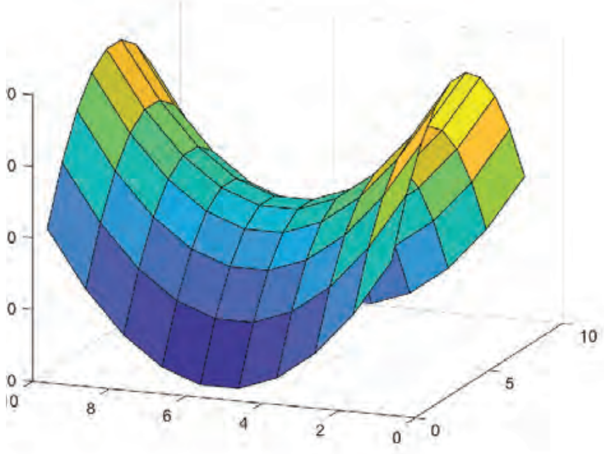

- Ponds connect through saddle points (Morse Theory).
- Red bond bond in percolation theory ~ saddle point.

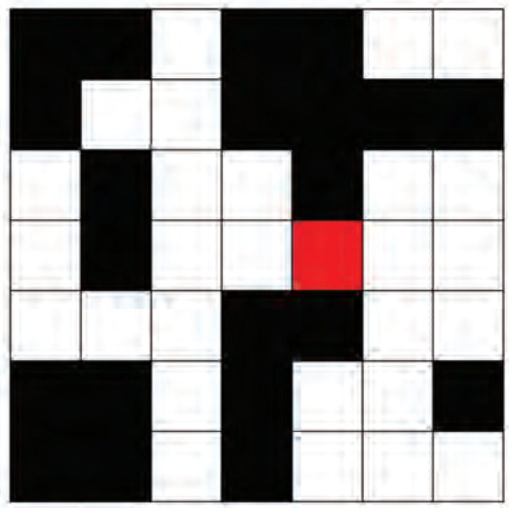

Evolution of Isoperimetric Quotient with Melt Pond Growth
(from real snow topography data)

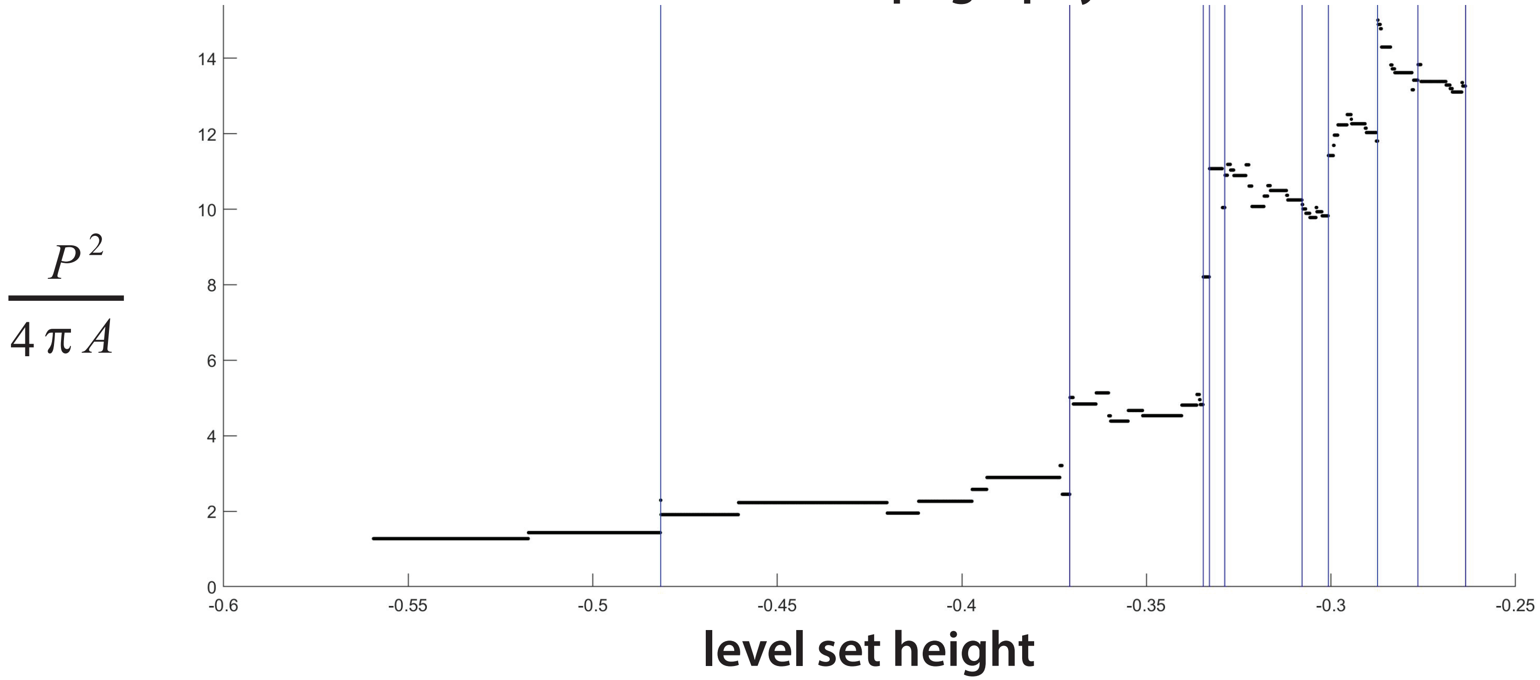

In the graph, we follow a single pond's growth. The vertical lines denote when the pond goes through a saddle point.

We see that large jumps in fractal dimension occur through saddle points.

pond coalescence and thickening

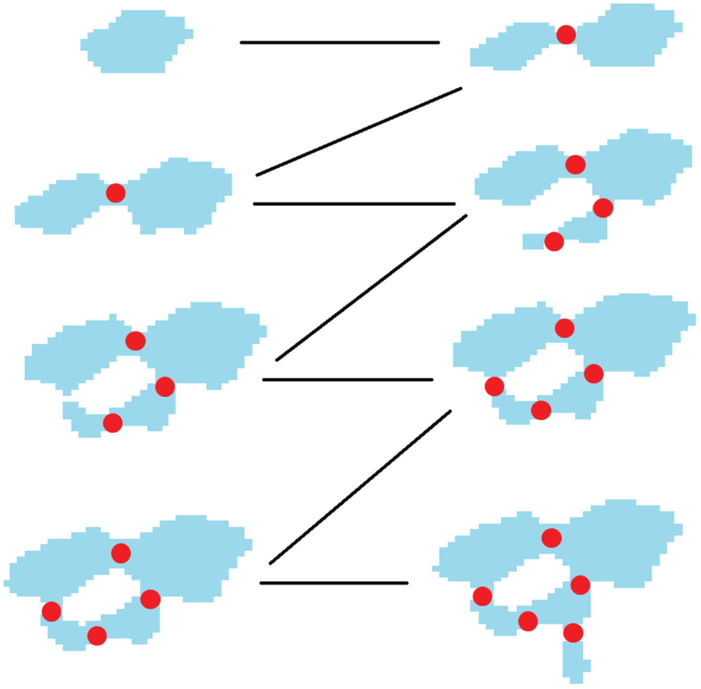

Ising Model for a Ferromagnet

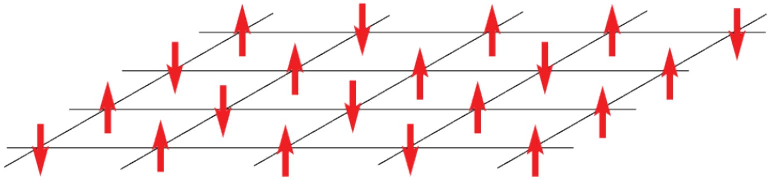

$$s_i = \begin{cases} +1 & \text{spin up} \\ -1 & \text{spin down} \end{cases}$$

blue

white

applied magnetic field

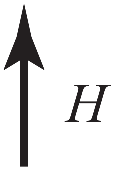

$$\mathcal{H} = -H \sum_i s_i - J \sum_{<i,j>} s_i s_j$$

nearest neighbor Ising Hamiltonian

ferromagnetic interaction $J \geq 0$

islands or ponds of like spins

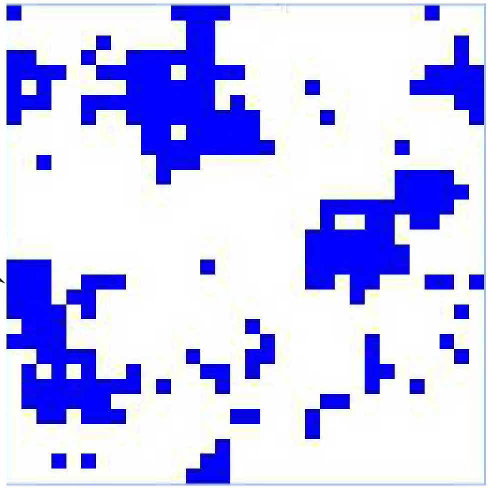

magnetization

$$M(T,H) = \lim_{N \to \infty} \frac{1}{N} \left\langle \sum_j s_j \right\rangle$$

homogenized parameter
like effective conductivity

Stieltjes integral representation for M

Baker, PRL 1968

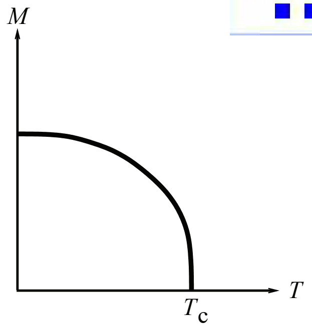

Curie point
critical temperature

Ising model for ferromagnets ⟶ Ising model for melt ponds

Ma, Sudakov, Strong, Golden, *New J. Phys.*, 2019

$$\mathcal{H} = -\sum_{i}^{N} H_i\, s_i - J \sum_{<i,j>}^{N} s_i s_j \qquad s_i = \begin{cases} \uparrow \quad +1 \quad \text{water} \quad \text{(spin up)} \\ \downarrow \quad -1 \quad \text{ice} \quad \text{(spin down)} \end{cases}$$

random magnetic field represents snow topography

magnetization M **pond coverage** $\dfrac{(M+1)}{2}$

~ albedo

only nearest neighbor patches interact

Starting with random initial configurations, as Hamiltonian energy is minimized by Glauber spin flip dynamics, system “flows” toward metastable equilibria.

Order from Disorder

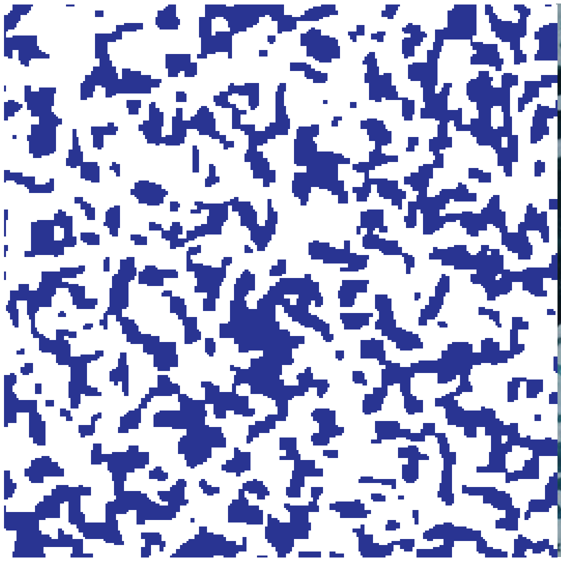

Ising model

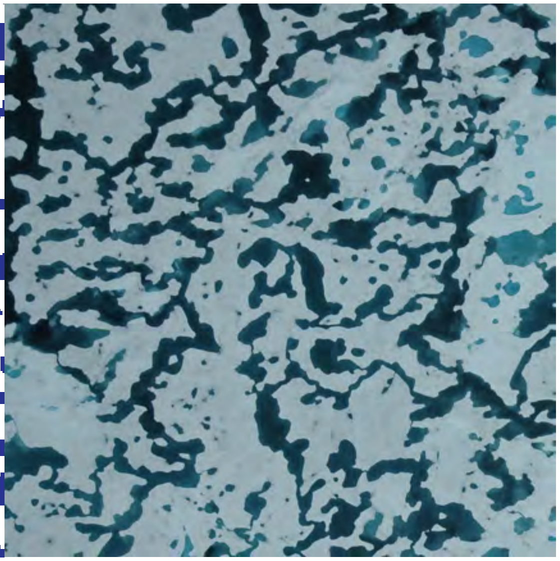

melt pond photo (Perovich)

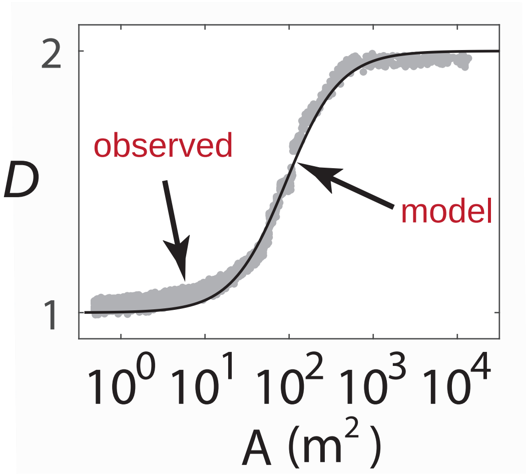

pond size distribution exponent

observed -1.5

(Perovich, *et al.* 2002)

model -1.58

ONLY MEASURED INPUT = LENGTH SCALE (GRID SIZE) from snow topography data

2011 massive under-ice algal bloom

Arrigo et al., *Science* 2012

melt ponds act as

WINDOWS

allowing light through sea ice

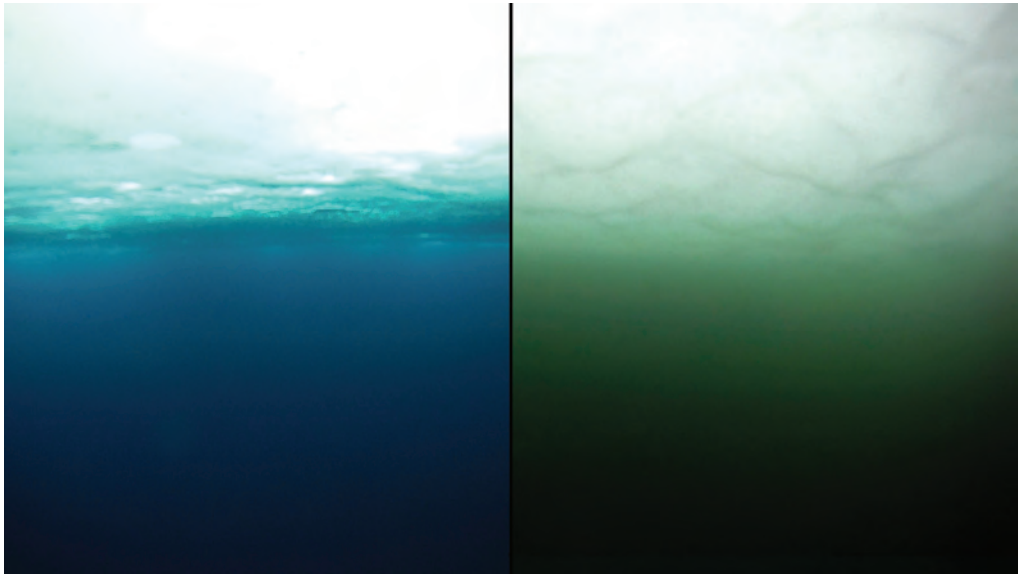

no bloom

bloom

Have we crossed into a new ecological regime?

The frequency and extent of sub-ice phytoplankton blooms in the Arctic Ocean

Horvat, Rees Jones, Iams, Schroeder, Flocco, Feltham, *Science Advances*, 2017

(2015 AMS MRC, Snowbird)

The effect of melt pond geometry on the distribution of solar energy under ponded first-year sea ice

Horvat, Flocco, Rees Jones, Roach, Golden, *Geophys. Res. Lett.*, 2020

- Model for 3D light field under ponded sea ice.

- Distribution of solar energy at depth influenced by ***shape and connectivity*** of melt ponds, as well as area fraction.

- Aggregate properties of the sub-ice light field, such as a significant enhancement of available solar energy under the ice, are controlled by parameter closely related to pond fractal geometry.

- Model and analysis explain how melt pond geometry ***homogenizes*** under-ice light field, affecting habitability.

Pond geometry affects the ecology of the Arctic Ocean.

The Melt Pond Conundrum:

How can ponds form on top of sea ice that is highly permeable?

C. Polashenski, K. M. Golden, D. K. Perovich, E. Skyllingstad, A. Arnsten, C. Stwertka, N. Wright

Percolation Blockage: A Process that Enables Melt Pond Formation on First Year Arctic Sea Ice

J. Geophys. Res. Oceans 2017

2014 Study of Under Ice Blooms in the Chuckchi Ecosystem (SUBICE)
aboard USCGC Healy

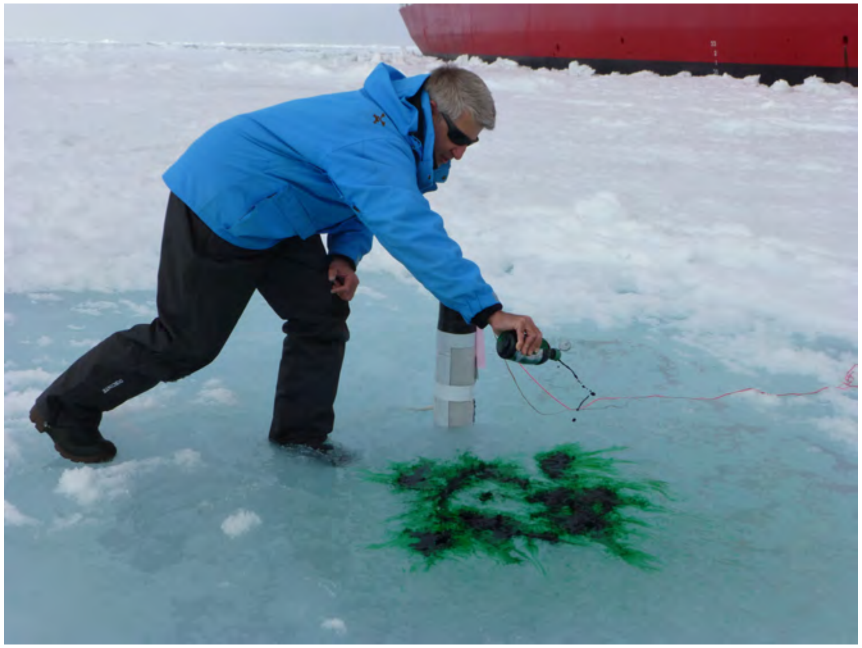

Conclusions

1. Sea ice is a fascinating multiscale composite with structure similar to many other natural and man-made materials.

2. Mathematical methods developed for sea ice advance the theory of composites and inverse problems in general.

2. Homogenization and statistical physics help ***link scales in sea ice and composites***; provide rigorous methods for finding effective behavior; advance sea ice representations in climate models.

3. Fluid flow through sea ice mediates melt pond evolution and many processes important to climate change and polar ecosystems.

5. Field experiments are essential to developing relevant mathematics.

6. Our research will help to improve projections of climate change, the fate of Earth's sea ice packs, and the ecosystems they support.

THANK YOU

Office of Naval Research

Applied and Computational Analysis Program

Arctic and Global Prediction Program

National Science Foundation

Division of Mathematical Sciences

Division of Polar Programs

UNITED STATES COAST GUARD

DEPARTMENT OF THE NAVY
ONR
Science & Technology

MCRN
Mathematics and Climate Research Network

Australian Government
Department of the Environment and Water Resources
Australian Antarctic Division

ace
CRC
ANTARCTIC CLIMATE & ECOSYSTEMS
COOPERATIVE RESEARCH CENTRE

NSF

Antarctica New Zealand

UAF
UNIVERSITY OF ALASKA FAIRBANKS

THE UNIVERSITY OF UTAH

Buchanan Bay, Antarctica   Mertz Glacier Polynya Experiment   July 1999

Two Layer Models and Effective Rheological Parameters

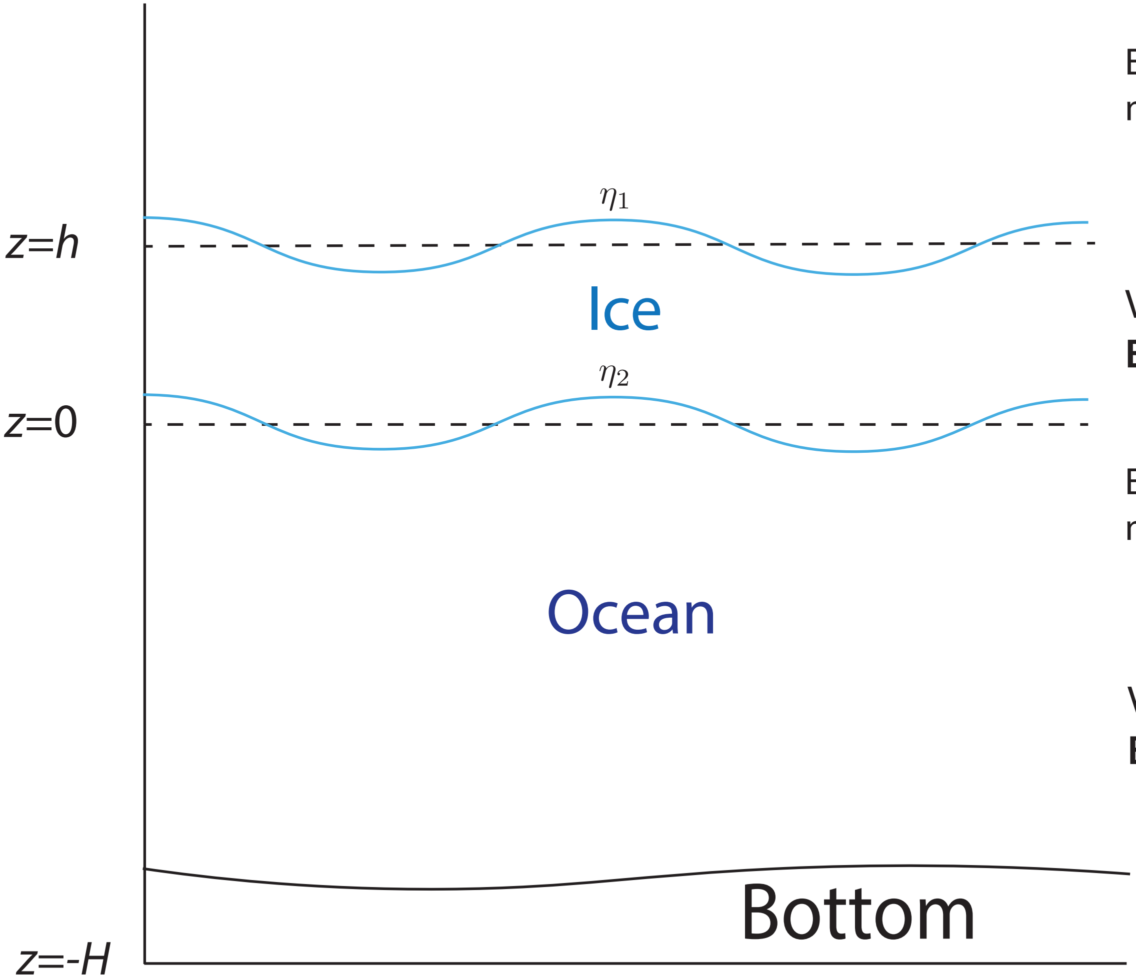

G shear modulus

P pressure

ω angular frequency

U velocity field

ν viscosity

λ Poission ratio

ρ density

g gravity

Viscous fluid layer (Keller 1998)

Effective Viscosity $\boxed{\nu}$

Equations of motion: $$\frac{\partial U}{\partial t} = -\frac{1}{\rho}\nabla P + \nu \nabla^2 U + g$$

Viscoelastic fluid layer (Wang-Shen 2010)

Effective Complex Viscosity $\boxed{\nu_e = \nu + iG/\rho\omega}$

Equations of motion $$\frac{\partial U}{\partial t} = -\frac{1}{\rho}\nabla P + \nu_e \nabla^2 U + g$$

Viscoelastic thin beam (Mosig *et al.* 2015)

Effective Complex Shear Modulus $\boxed{G_v = G - i\omega\rho\nu}$

Stieltjes integral representation for effective complex viscoelastic parameter; bounds

Sampson, Murphy, Cherkaev, Golden 2019

Homogenization for two phase viscoelastic composite

$\nu_1 = 10^7 + i\,4875$ **pancake ice**

$\nu_2 = 5 + i\,0.0975$ **slush / frazil**

microscale $\sigma = C_{ijkl}\epsilon_{kl} = C : \epsilon$

$$C = 2(\chi_1\nu_1 + \chi_2\nu_2)\Lambda_s$$

macroscale $\langle\sigma\rangle = C^* : \langle\epsilon\rangle$

$$\langle\epsilon\rangle = \epsilon^0$$

quasistatic assumption $\nabla \cdot \sigma = 0$

Tom Gill

Strain Field

$$\epsilon = \frac{1}{2}[\nabla u + (\nabla u)^T] = \nabla^s u \quad \nabla \cdot u = 0$$

Resolvent

$$\epsilon = \left(1 - \frac{1}{s}\Gamma\chi_1\right)^{-1}\epsilon^0 \Rightarrow \boxed{\frac{\nu^*}{\nu_2} = \left(1 - \|\epsilon^0\|^{-2}F(s)\right)}$$

$$F(s) = \int_0^1 \frac{d\mu(\lambda)}{s - \lambda} \qquad s = \frac{1}{1 - \frac{\nu_1}{\nu_2}}$$

$$\Gamma = \nabla^s(\nabla \cdot \nabla^s)^{-1}\nabla \cdot$$

Model Approximations

Floes $\approx$ Discs

Forces on Disc $= \quad F_{drag} + F_{collision}$

A. Herman ***Physical Review E*** **2011**

Floe-Floe Interactions: Linear Elastic Collisions

$F_{collision}$ follows Hooke's Law.

Advective Forcing: Passive, Linear Drag Law

v is the advective velocity field.

F_{drag} is proportional to relative velocity.

Ice Pack Characteristics

ϕ = sea ice concentration (floe area fraction)

Power Law Size Distribution: $N(D) \sim D^{-k}$

T. Toyota, S. Takatsuji, M. Nakayama Geophysical Review Letters 2006

k = floe diameter exponent

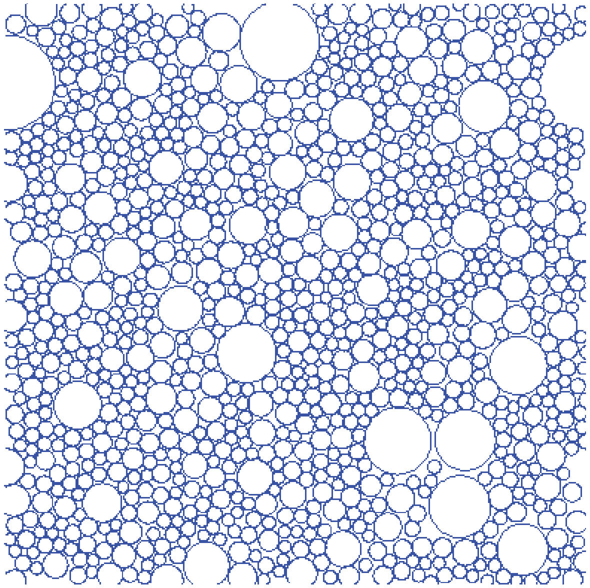

k = 2.9, ϕ = 0.8

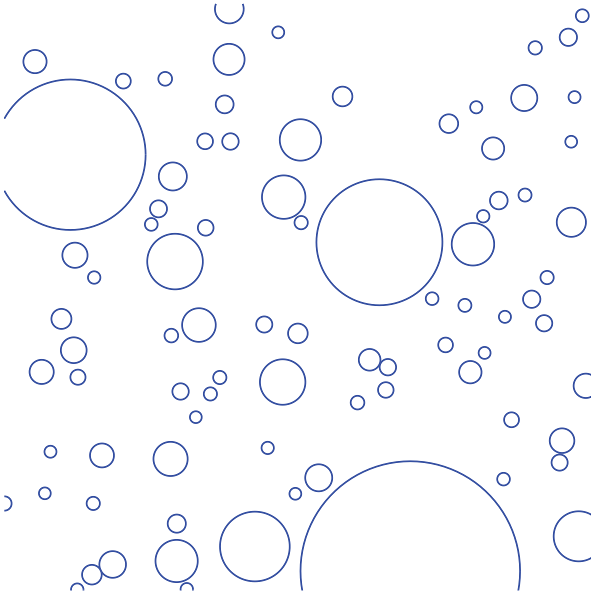

k = 1.7, ϕ = 0.1

Model Results

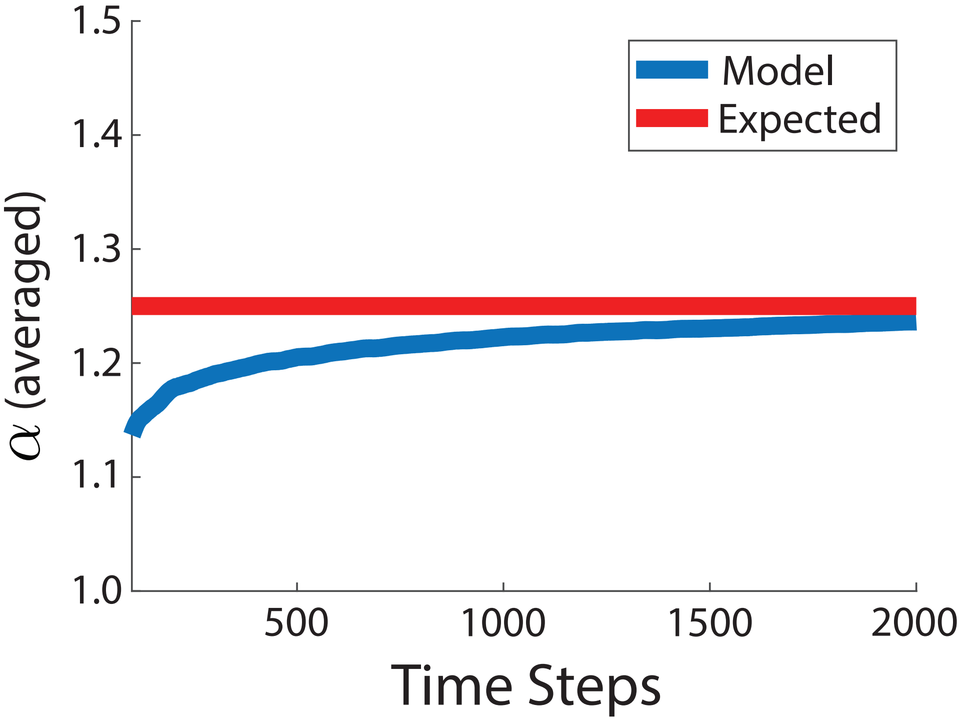

Sparse Packing, Shear Dominated Drift

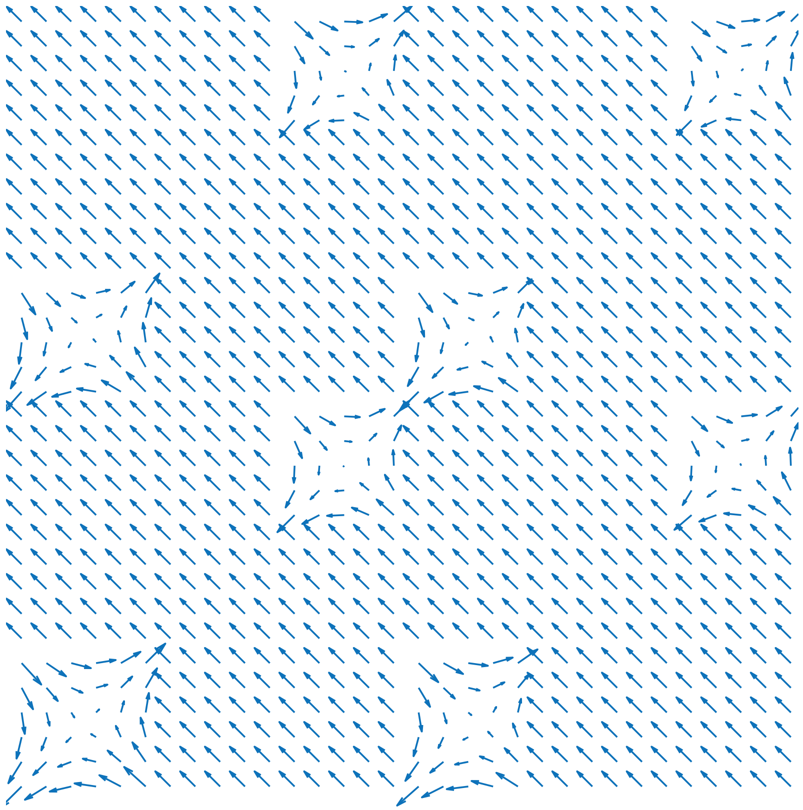

Expected $\alpha = 5/4$

k = 2.9 Concentration = 0.3